CHALMERS
UNIVERSITY OF TECHNOLOGY

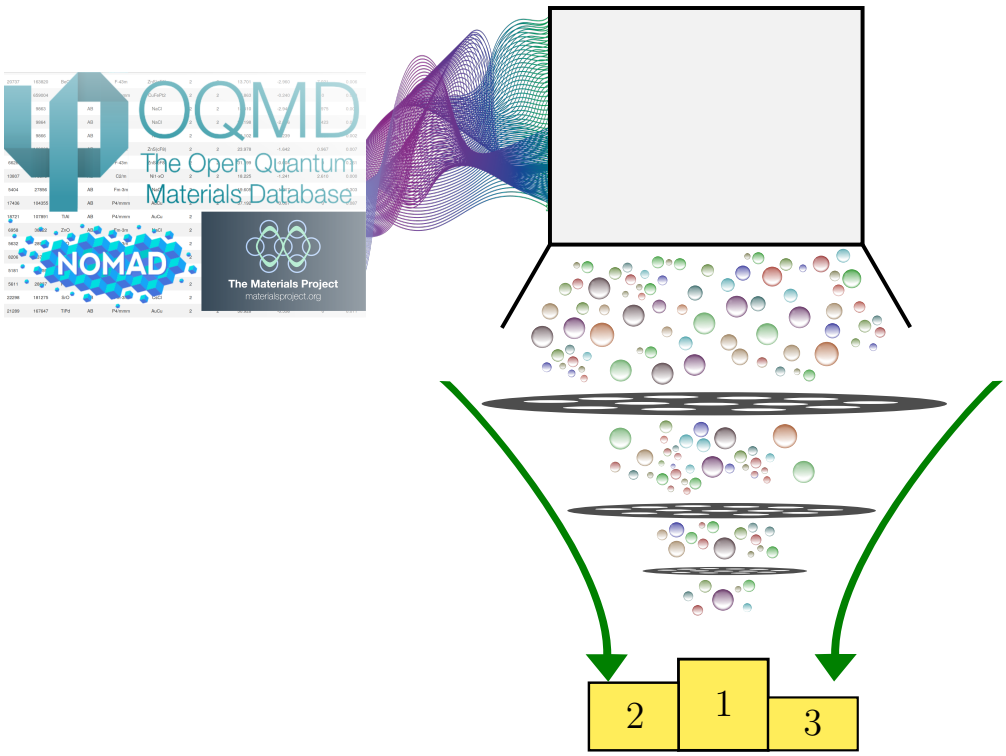

High-throughput in-silico screening of oxygen carrier candidates for chemical looping oxygen uncoupling

Thermodynamical and practical considerations of data mining from ab-initio databases — towards a cost-effective negative emission technology

Master's thesis in Applied Physics

VIKTOR REHNBERG

DEPARTMENT OF PHYSICS
Division of Chemical Physics

CHALMERS UNIVERSITY OF TECHNOLOGY
Gothenburg, Sweden 2020
www.chalmers.se

Master's thesis 2020

High-throughput in-silico screening of oxygen carrier candidates for chemical looping oxygen uncoupling

Thermodynamical and practical considerations of data mining from ab-initio databases — towards a cost-effective negative emission technology

Viktor Rehnberg

CHALMERS
UNIVERSITY OF TECHNOLOGY

Department of Physics
Division of Chemical Physics
Chalmers University of Technology
Gothenburg, Sweden 2020

High-throughput in-silico screening of oxygen carrier candidates for chemical looping oxygen uncoupling
Thermodynamical and practical considerations of data mining from ab-initio databases — towards a cost-effective negative emission technology
Viktor Rehnberg

Supervisor: Adam Arvidsson, Department of Physics
Examiner: Anders Hellman, Department of Physics

Master's Thesis 2020
Department of Physics
Division of Chemical Physics
Chalmers University of Technology
SE-412 96 Gothenburg
Telephone +46 31 772 1000

Cover: A schematic of the workflow of the proposed screening methodology. Data comes from ab-initio databases and transformed into all possible phases and associated phase transitions, that then pass through different filters. Finally, the remaining phase transitions are ranked according to e.g. cost and oxygen transfer capacity.

Typeset in LaTeX
Printed by Chalmers Digitaltryck
Gothenburg, Sweden 2020

High-throughput in-silico screening of oxygen carrier candidates for chemical looping oxygen uncoupling
Thermodynamical and practical considerations of data mining from ab-initio databases — towards a cost-effective negative emission technology

Viktor Rehnberg
Department of Physics
Chalmers University of Technology

Abstract

It is clear that different techniques of carbon capture and storage will prove to be important in achieving the current global climate goals. One such technique is combustion of biofuel with chemical looping combustion or chemical looping oxygen uncoupling (CLOU). These are techniques where a metal oxide is used as an intermediary to transport oxygen between a chamber with an air inlet to a chamber with a fuel inlet. In CLOU the metal oxide is oxidised in the air chamber and then transports the extra oxygen to the fuel chamber. Thanks to the low partial pressure of oxygen in the fuel chamber the metal oxide is reduced and releases the extra oxygen. This oxygen in gaseous state will then react with the fuel and thus the partial oxygen pressure in the fuel chamber remain low. The metal oxide can continue looping through the two chambers transporting oxygen. As only oxygen and fuel are present in the combustion the only exhaust gases under full combustion are carbon dioxide and water. No toxic oxides of nitrogen are produced and expensive post-combustion gas separation of nitrogen and other flue gases can be avoided. The water can easily be separated by condensation and the carbon dioxide can then be captured cheaply and later stored in, for instance, geological formations underground.

This report proposes a new method based on using the bountiful data from ab-initio databases, for instance available in the Open Quantum Materials Database, to propose possible candidates for oxygen carriers in chemical looping oxygen uncoupling (CLOU). The data, in this case formation energy at 0 K and 0 Pa, is extrapolated based on thermodynamic considerations to find the stable phases of oxygen carriers under realistic conditions used for CLOU. Further considered criteria include mainly cost, toxicity and oxygen transfer capacity. A quantitative summary of all the considered criteria is proposed and also used to list potential metal oxide oxygen carriers in the order of how promising they seem for CLOU. The list can be used to guide what experimental investigations should prioritise, thus, it has the potential to significantly speed up the search for better oxygen carriers.

Keywords: chemical looping, material screening, data mining, Ellingham diagram, thermodynamics.

Acknowledgements

I would like to thank Adam Arvidsson and Anders Hellman for the insightful discussions, guidance and expectations that led this project to conclusion. Without them this thesis might have gone in any direction.

I would also like to extend my thanks to Henrik Leion, Tobias Mattisson, Rizwan Raza, Yongliang (Harry) Yan and Arijit Biswas for sharing their insights into the experimental side of things as well as for their insightful questions that led me to refine the material further. You have led me to realise how both breadth and depth can gain from a multidisciplinary approach.

Last but not least, I am grateful to Emelie for her proofreading and emotional support.

Viktor Rehnberg, Gothenburg, June 2020

Contents

List of Figures

List of Tables

Glossary

ASE Atomic Simulation Environment. xiii, 27

CL chemical looping. xi, 2, 5–7, 13, 19, 20, 22, 33, 39, 41

CLC chemical looping combustion. 1, 19, 22

CLOU chemical looping oxygen uncoupling. xi–xiii, 1–3, 6, 14, 19, 20, 22–26, 29, 30, 33–35, 37, 39, 41

DFT density functional theory. 2, 5, 9, 10, 13, 15, 17

OC oxygen carrier. xi, xii, 1–3, 5–8, 13, 19, 22–26, 29, 30, 32–34, 39–41

OQMD Open Quantum Materials Database. xi, 3, 10, 14, 21, 29, 41

RMSE root mean square error. xiii, 36, 38

Vasp Vienna Ab initio Simulation Package. xiii, 27

Chapter 1

Introduction

The atmospheric conditions are one of the key conditions for the existence of life as we know it on earth. However, carbon dioxide and other greenhouse gases that mankind has released into the atmosphere have already started changing these conditions, causing a global heating effect. There exist international commitments to stop or slow this global heating, one of the best known of these commitments is what is commonly called the Paris Agreement. In the Paris agreement, that was reached at the 21st annual Conference of the Parties, the Parties recognized: "the need for an effective and progressive response to the urgent threat of climate change on the basis of the best available scientific knowledge," (United Nations [1])

One of the key points that were agreed upon was to limit the increase in global average temperature to well below 2 °C and aiming for no more than 1.5 °C above preindustrial levels [1]. This agreement between 189 parties signify a landmark in global mitigation of climate heating.

When investigating the possible scenarios in which the Paris agreement goal of limiting global climate heating to 2 °C or 1.5 °C, the need for carbon dioxide removal by way of bio-energy with carbon capture and storage has been identified [2–9]. This means that the carbon dioxide removal is achieved by burning bio mass and then collecting and storing the carbon dioxide released from the process. However, if burnt in air it will be problematic or expensive to separate the oxygen from the flue gas [10].

One combustion technique that avoids this problem associated with post-combustion processes, is combustion through chemical looping combustion (CLC) or chemical looping oxygen uncoupling (CLOU) [11–19]. These techniques work by separating the combustion process into two steps separated in different chambers with metal oxides as intermediaries. In one chamber, air is allowed and the metal oxide is oxidised. This is the air chamber. In the other chamber, fuel is introduced and here the metal oxide is reduced and the released oxygen reacts with the fuel. This way the exhaust gases from the fuel chamber are carbon dioxide and water. As water can easily be separated by condensation this process avoids expensive post-combustion separation of carbon dioxide from the other flue gases.

The properties of the metal oxide that is transporting oxygen from the air chamber to the fuel chamber is important for the process. However, experimental investigations into the right oxygen carriers (OCs) can be time consuming [20]. When con-

sidering combinations of several different elements the elements investigated would have to be a small subset of the all chemical elements, as not to be overcome by the combinatorics. This thesis will instead investigate a method for fast in-silico screening of materials that could be relevant for CLOU.

Ab-initio methods such as density functional theory (DFT) have seen much use in computational physics for investigating electronic structures properties of materials [21]. The electronic structure properties will in turn tell a lot about a materials properties [22]. However, DFT can be computationally demanding and performing all the calculations for a high throughput investigation for unknown structures would become quite costly. Luckily there exist a number of databases with DFT data [23–28] that can be used instead.

1.1 Scope

This thesis has one main problem statement: how can in-silico methods be used for a faster screening of OCs for CLOU?

There are other chemical looping (CL) processes than CLOU that could benefit for a similar technique. The reason that CLOU was chosen was that in CLOU the OC releases oxygen in the fuel chamber regardless of what fuel is used and this reduces the number of things to consider. Furthermore, with CLOU the kinetics in the reactions could potentially become significantly less important and only thermodynamics could and will be considered.

Beyond the main problem statement a number of further questions naturally arises. What constitutes the criteria for a good OC? How could these criteria be quantified and later used to rank the possible OC after potential usefulness?

While most of the attributes that are relevant for OC in the CLOU process there is one step that will not be investigated in depth. The physical stability of the metal oxide, i.e. the tendency for attrition and agglomeration of the metal oxide including melting point. No computationally cheap universal measure for this has been acquired and this property will have to be investigated in experiments or further theoretical studies.

1.2 Outline

Investigations of possible OCs are often done by experiment and can be time consuming. This report introduces a method by which existing data from existing ab-initio databases can be used to screen for possible OCs at a much higher rate.

In chapter 2 the underlying theory of CL processes are examined a bit closer and some of the underlying theory for the physics in the problem is presented.

In chapter 3 some expressions are derived and the workflow is presented. Using formation energies at 0 K and 0 Pa from ab-initio databases and considering temperature and pressure dependence of the chemical potential of oxygen a way to find the thermodynamically stable phases at different conditions is described. This can in turn be used to find out if a material will be oxidised in the air chamber and reduced in the fuel chamber, which is a key criteria for OCs.

However, when considering possible OCs, whether they work in the intended chemical process is not the only criteria to consider. There are other more practical considerations that could be taken into account, e.g. toxicity, price, oxygen transfer capacity etc. A method for reducing the possible OC candidates and rank the possible OCs after their potential usefulness is introduced as well.

In chapter 4 data from the Open Quantum Materials Database (OQMD) is used to produce a ranking of potential candidates and the top candidates as well as some of the milestones in the workflow are presented. The accuracy of the results is discussed.

Lastly, in chapter 5 implications of the underlying assumptions are considered as well as how future research could be performed. This thesis has contributed to a novel methodology for high-throughput screening of promising candidates for CLOU with a quantitative measure of each metal oxide that can be used for ranking the metal oxides at hand.

Chapter 2

Theoretical background

This chapter will explore what is known about CL processes and how the problem scales when polymetallic compounds are considered. Furthermore, basics of thermodynamics and what the ab-initio method DFT is all about is summarised. Two previous approaches to the thermodynamics are presented as well. These will be compared to the developed methodology in later chapters.

2.1 Principles of Chemical Looping

The main idea behind CL is that a chemical reaction can be divided into separated successive reactions [11]. In the paper where Ishida, Zheng, and Akehata [11] first coined the term "chemical looping", the reaction that was considered was

$$\mathrm{CH_2} + 2\mathrm{O_2} \leftrightharpoons \mathrm{CO_2} + 2\mathrm{H_2O}\,,$$

which was separated into combustion of the fuel by reducing an OC

$$\mathrm{CH_2} + 4\mathrm{MeO} \leftrightharpoons \mathrm{CO_2} + 2\mathrm{H_2O} + \mathrm{Me}\,,$$

and reoxidising the OC

$$2\mathrm{MeO} \leftrightharpoons 2\mathrm{Me} + \mathrm{O_2}.$$

To enable this separation of reactions a metal oxide acting as an OC is introduced to the process. In practice the separation consists of physically separating the chemical processes in different reaction chambers and allowing only the OC to travel between them.

Initially CL was thought of as a new combustion technique with potential for an increased efficiency [11], the potential with respect to environmental aspects was considered seven years later [12]. When using CL for combustion of a hydrocarbon fuel the exhaust gas consist of only carbon dioxide and water, see fig. 2.1. There are for example no nitrogen oxides as the combustion takes place in an environment without nitrogen, as compared to direct combustion in air. Furthermore, if the water is removed by condensation only carbon dioxide remains to be captured and stored. Hence, there are little or no greenhouse gas emissions released from the process.

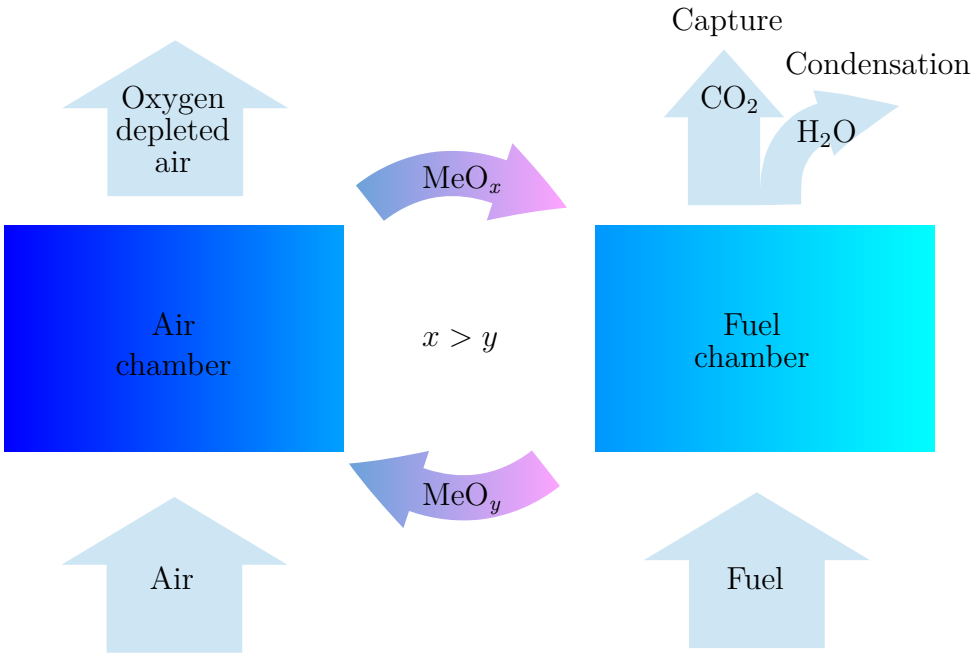

Figure 2.1: *Schematic of the idea behind CL for combustion. In the air chamber where the OC is oxidised the input is air and the output is simply oxygen deficient air. In the fuel chamber the OC is reduced by the fuel that is coming in and out goes carbon dioxide and water. The water can easily be separated from the carbon dioxide by condensation.*

In the time since the initial work by Ishida et al. (see e.g. [11, 12]), CL have been realised for many other applications [14, 16, 29], see fig. 2.2. Though, this Master's thesis will mainly focus on a special kind of CL that can be used for combustion, namely CLOU, the results could be adapted somewhat to other forms of CL processes if one knows the characteristics of the fuel.

It is easily realised that the CL process will be heavily determined by the performance of the metal oxide that acts as an OC. The key criteria for an oxygen carrier in a CL process is to be able to transport a chemical species from one chamber to the other chamber, leave it there and return to the first chamber for another loop. In combustion applications the transported chemical species is oxygen and the metal oxide acting as an OC should be oxidised in the chamber were the air inlet is (the air chamber) and be reduced in the chamber were the fuel inlet is (the fuel chamber).

In practical applications a fluidised bed reactor system can be used [17, 19]. The principle behind a fluidised bed reactor is that there is some solid bed material consisting of grains in the order of 100 µm to a few mm [30] and by flowing a gas through this the bed material, it becomes free flowing, similar to a fluid. This has implications for the desired properties of the OC.

According to Lyngfelt [31] important criteria for OCs in CL for combustion, are that they should:

- have high reactivity with fuel and oxygen;
- convert the fuel fully to carbon dioxide and water;

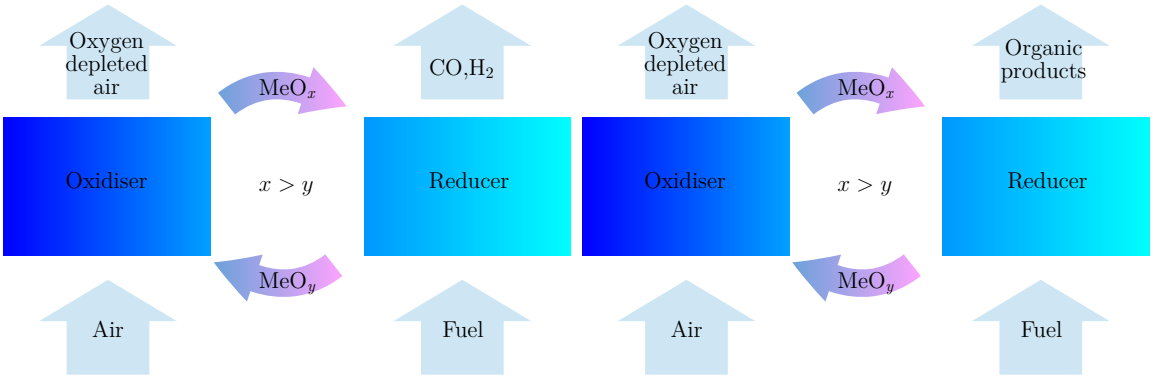

(a) *Chemical looping partial oxidation. The fuel is a hydrocarbon.*

(b) *Chemical looping selective oxidation. The fuel is a hydrocarbon.*

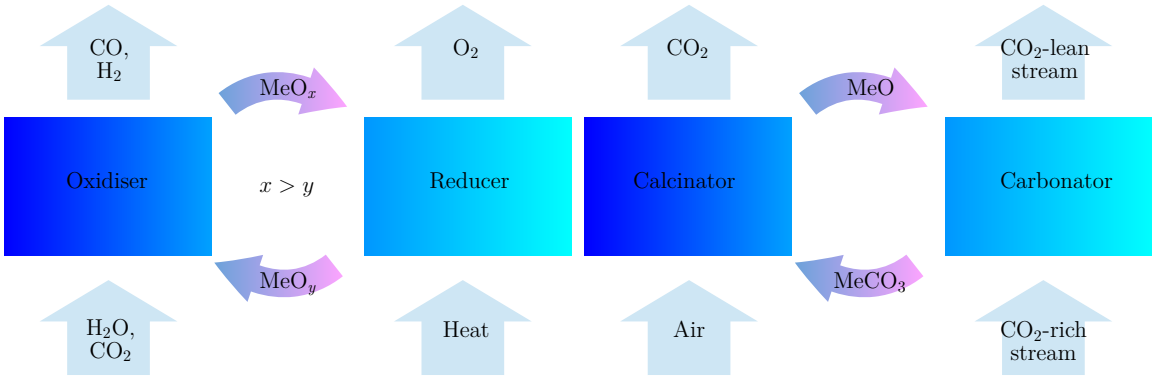

(c) *Thermochemical water/carbon dioxide splitting with chemical looping.*

(d) *Chemical looping carbon capture.*

Figure 2.2: *Some applications of CL beyond full combustion. The figure was adapted from Zeng et al. [14].*

- not break or stick together too much;
- be cheap;
- not compromise health or safety;
- be able to transport a sufficient amount of oxygen.

This thesis touches upon all of the mentioned criteria. However, the physical stability of the OCs will not be considered beyond a rough estimate of melting points, this will have to be considered either experimentally or in further theoretical studies.

2.2 Combining elements and the combinatorial explosion

When searching for OCs the possibilities increase when also considering alloys with more than one element. However, this makes the scope of the problem a lot larger as well. Consider that you would like to consider n elements and you would like to allow up to k different elements per compound. Then the number of possible combinations are

$$N_{\text{combinations}} = \sum_{k_i=1}^{k} \binom{n}{k} .$$

Furthermore, suppose that there exist phases with ten unique ratios of elements for each combination and that you would like to consider all combinations that could work for each ratio of elements. The number of such combinations are roughly then on the order of 10^{k_i} which gives

$$N_{\text{ratio combinations}} \sim \sum_{k_i=1}^{k} \binom{n}{k} \cdot 10^{k_i} .$$

This kind of back-of-the-envelope calculation gives for 100 elements and phases with up to three elements in each phase

$$N_{\text{ratio combinations}} \sim \frac{100^3}{3!} \cdot 10^3 \sim 10^8 . \tag{2.1}$$

It becomes apparent that the computational complexity for each such combination of phases must be kept low.

2.3 Key thermodynamical quantities

Some previous knowledge of thermodynamics is assumed, however this section will repeat some of the key quantities necessary to understand this thesis.

We can define Gibbs potential or Gibbs free energy as

$$G = U + pV - TS , \tag{2.2}$$

where U is the internal energy of a system, p is the pressure, V is the volume, T is the temperature and S is the entropy [32]. This quantity will be a useful concept for us as an implication of the second law of thermodynamics is that Gibbs free energy is minimised at thermodynamic equilibrium [33]. The entropy S is connected to the number of possible micro-states of the system by the Boltzmann-Planck equation [34, p. 41]

$$S = k_{\text{B}} \log(\Omega) , \tag{2.3}$$

where Ω is the number of (equiprobable) microstates and $k_{\text{B}} = 8.6 \times 10^{-5}\,\text{eV/K}$ is the Boltzmann constant.

Other useful quantities are the specific heat at constant volume [35, Ch. 45]

$$C_V = \left(\frac{\partial U}{\partial T}\right)_V , \tag{2.4}$$

and the chemical potential [32]

$$\mu_\gamma = \left(\frac{\partial G}{\partial n_\gamma}\right)_{T,p,\gamma'\neq\gamma} . \tag{2.5}$$

The specific heat is related to how the internal energy changes with temperature and the chemical potential relates how the Gibbs free energy changes with amount of some chemical species γ.

The pressure dependence of the chemical potential was derived by Reuter and Scheffler [36] and is

$$\mu_{O_2}(T,p) = \mu_{O_2}(T,p_0) + k_B T \log\left(\frac{p}{p_0}\right), \tag{2.6}$$

where p_0 is a reference partial oxygen pressure for which the chemical potential of oxygen is known. Furthermore, to get the chemical potential at some particular oxygen pressure the relation

$$\mu_{O_2}(T,p_0) = H_{O_2}(T,p_0) - H_{O_2}(0\,\mathrm{K},p_0) - T(S_{O_2}(T,p_0) - S_{O_2}(0\,\mathrm{K},p_0)) , \tag{2.7}$$

can be used [36]. Here the enthalpy of oxygen H_{O_2} and entropy of oxygen S_{O_2} could be found through e.g. experimental tables.

2.4 Quantum mechanics and Density Functional Theory

The main contributions toward DFT build on foundations of quantum physics such as the Schrödinger equation [37] and were made by Hohenberg and Kohn [38], and Kohn and Sham [39]. For those in the field, the revolutionary ideas of DFT can be provoking:

> Density-functional theory (DFT) is a subtle, seductive, provocative business. Its basic premise, that all the intricate motions and pair correlations in a many-electron system are somehow contained in the total electron density alone, is so compelling it can drive one mad. (Becke [21])

The first part of the name "density functional theory" comes from working with the density rather than the wavefunction and the second part comes from that this is done through a functional, e.g. the energy can be described as a functional of the total electron density

$$E = E[n] .$$

While in principle an exact method, the exact functional is not known and instead approximations are used [22, 40, 41]. As such, knowing the accuracy of the calculations is important and estimates have been made. When comparing with experiment a commonly used functional by Perdew, Burke, and Ernzerhof [42] (PBE) was estimated to have a mean absolute error of 0.35 eV for molecules and 0.16 eV for solids [43]. Furthermore, the Hubbard model can be used to extend DFT in to what is known as DFT+U, to increase the accuracy of the description of strong on-site Coulomb interaction of localised electrons [44–46]. This is especially relevant for metal oxides.

To avoid any systematic errors Kirklin et al. [27] applied some further methods for the entries in the OQMD database. A variant of the Fitted Elemental Reference Energies method [47] was applied in which the chemical potential of 13 elemental species whose DFT predicted groundstates were known to differ from elemental chemical potentials corresponding to standard temperature and pressure phases. With this approach Kirklin et al. [27] report that their mean absolute error is 0.096 eV/atom when compared to experiments.

The formation energies acquired through DFT are for 0 K temperature. In chapter 3 a way to extend these energies to higher temperatures is presented. However, these derivations will be done by neglecting most of the differences in temperature dependence between compounds. Another way to take temperature dependence into account would be by taking the phonon contribution to the DFT energies into account.

Alfè [48] describes a method called the small displacement method which estimates the phonon contribution by calculating the force coefficient matrix by calculating the forces from small displacements of an atom at the time (small enough to be in the region were the forces are proportional to the displacement). Furthermore, Alfè [48] show that this can be used to calculate the phonon dispersions. Which can in turn be used to calculate Helmholtz energy at different temperatures using the partition function for a crystalline solid [49, Ch. 11].

2.5 Shomate equation

This project will be based on theoretical data. However, approaches based on experimental data exist and one such representation is through the Shomate equation

$$
\begin{aligned}
S(t) &= A\log(t) + Bt + C\frac{t^2}{2} + D\frac{t^3}{3} - \frac{E}{(2t^2)} + G\,,\\
H(t) &= At + B\frac{t^2}{2} + C\frac{t^3}{3} + D\frac{t^4}{4} - \frac{E}{t} + F\,,\\
t &= \frac{T}{1000\,\mathrm{K}}\,,
\end{aligned}
$$

where parameters $A \ldots G$ are fitted to experiments in some temperature region, T is temperature and S and H are standard entropy and standard enthalpy respectively. The parameters can be found from the NIST-JANAF themochemical tables [50].

This can of course be expanded to the Helmholtz free energy

$$F = H - TS\,,$$

which is related to the Gibbs free energy through the expansion work

$$G = H + pV - TS\,.$$

Chapter 3

Methods

In an attempt to find potential OC candidates for CL, the first step will be to consider what information that is available from theory. For this quantum mechanics and the formalism of DFT was investigated in section 2.4. However, the computational cost of DFT will be quite limiting, luckily there exist databases with DFT data [23–28]. To use this data we will consider what part of the data that is available in the databases that can be used.

The next step will be to see how this data can be used for our original goal in finding OC candidates. We will consider equilibrium states (i.e. thermodynamics) to find stable phases and corresponding phase transitions. With this we will explore what we can say about some materials usability as an OC in CL processes.

The final step will be to consider how the information gained can be controlled for its validity. We will consider how the impacts of some of the assumptions can be investigated theoretically. Furthermore, we will consider how comparisons can be made with experimental data and some of the challenges corresponding to this.

The development of the codebase for the project has been in primarily Python 3.7 [51]. Many of the numerical calculations have been utilising the NumPy [52] and SciPy [53] packages. Python generated figures have mainly been created with Matplotlib [54], Seaborn [55] and Tikzplotlib [56] and the tables were generated by Pandas [57].

3.1 Overview of workflow

A brief sketch of the workflow can be found in fig. 3.1. First data from some database will be combined to create the full space of possible compounds and mixes of materials, then these will go through thermodynamic considerations and filtered on practical aspects. Finally, the remaining candidates can be ranked according to the ranking system established in section 3.10.

3.2 Choosing database

For exploring the possibilities of the projects methodology, the choice of database was not vital. Key criteria that came into the choice was the need for some kind

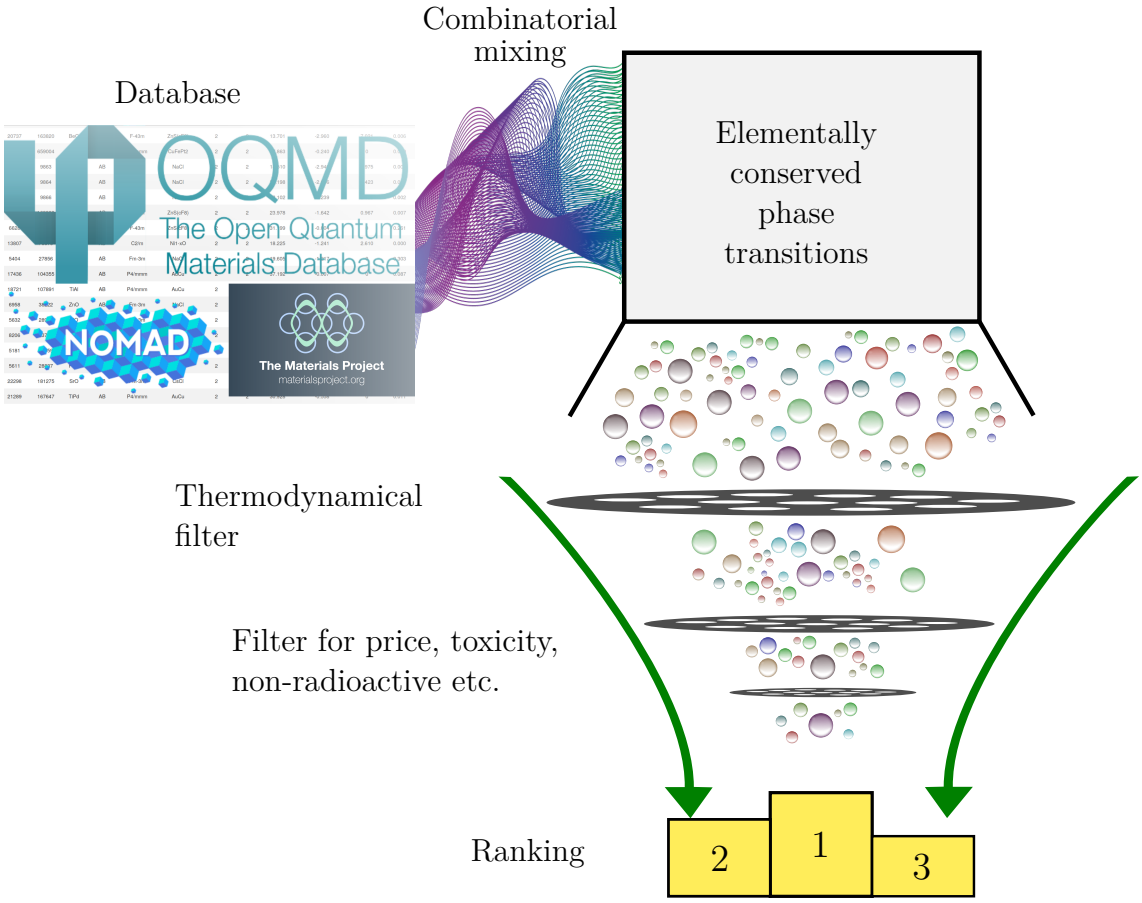

Figure 3.1: *The overall workflow for the process. Starting from database and ending with promising candidates ready for validation. The spheres symbolise candidates for CLOU. In actuallity only the OQMD was used. However, other could have been used and this is illustrated by including the Novel Materials Discovery (NOMAD) Laboratory [23] and the Materials Project [28].*

of simple interface to acquire data from the database and a large amount of data. The database that was chosen was the OQMD [26, 27]. However, the development has not been contingent upon this choice and can presumably be adapted to any other database with formation energies. Either some other theoretical database (e.g. [23–25, 28]) or from experimental data.

3.3 Estimating Gibbs free energy of formation

Considering Gibbs free energy from eq. (2.2)

$$G = U + pV - TS\,,$$

where U is the internal energy, p is the pressure, V is the volume, T is the temperature and S is the entropy. For the transition of pure metal to a pure metal oxide

[58]

$$x\,\mathrm{Me} + \mathrm{O_2} \leftrightharpoons \mathrm{Me}_x\mathrm{O_2}\,.$$

the Gibbs free energy of formation was defined for the metal oxide as the change in Gibbs free energy when going to the metal oxide from the most stable phases of the constituents is

$$G_{f,\mathrm{Me}_x\mathrm{O_2}} = G_{\mathrm{Me}_x\mathrm{O_2}} - xG_{\mathrm{Me}} - G_{\mathrm{O_2}}\,. \tag{3.1}$$

The reason that the Gibbs free energy of formation was considered was that the thermodynamically most stable phase is the one that minimises Gibbs free energy of formation [33].

Most DFT databases contain the internal energy at 0 K and 0 Pa, i.e. $U_f(T = 0\,\mathrm{K}, p = 0\,\mathrm{Pa})$. Gibbs free energy at 0 K and 0 Pa is then

$$\begin{aligned} G_f(T = 0\,\mathrm{K}, p = 0\,\mathrm{Pa}) &= U_f(T, p) + \Delta_f(pV) - TS_f \\ &= U_f(T = 0\,\mathrm{K}, p = 0\,\mathrm{Pa})\,. \end{aligned} \tag{3.2}$$

To get the temperature and pressure dependence, contributions from the oxygen and metals were considered separately.

Considering the chemical potential from eq. (2.5)

$$\mu_\gamma = \left(\frac{\partial G}{\partial n_\gamma}\right)_{T,p,n_{\gamma'\neq\gamma}}\,,$$

this corresponds to change in free energy for a small change in amount of substance of some species γ. Therefore,

$$G_{\mathrm{O_2}}(T, p) = G_{\mathrm{O_2}}(T = 0\,\mathrm{K}, p = 0\,\mathrm{Pa}) + n_{\mathrm{O_2}}\mu_{\mathrm{O_2}}\,. \tag{3.3}$$

As for metals, the volume per atom is around $10\,\mathrm{Å}^3$/atom to $50\,\mathrm{Å}^3$/atom [26] and varies slowly with temperature an pressure [59]. This gives

$$pV \sim 10^5\,\mathrm{Pa} \cdot 20\,\mathrm{Å}^3/\mathrm{atom} \sim 10^{-5}\,\mathrm{eV/atom}\,,$$

which will be even smaller when considering differences. Therefore, the $\Delta_f(pV)$-term will be neglected.

Furthermore, for the metallic phases the volume was assumed to be vary slowly with pressure and temperature [59]. With this the specific heat at constant volume from eq. (2.4) could be used

$$C_V = \left(\frac{\partial U}{\partial T}\right)_V\,.$$

This gives

$$U(T, p) = U(T = 0\,\mathrm{K}, p = 0\,\mathrm{Pa}) + \int_{0\,\mathrm{K}}^{T} C_V(T')\,\mathrm{d}T'\,. \tag{3.4}$$

As for the temperature dependence on Gibbs free energy from entropy TS, any contribution to the Gibbs free energy was neglected except one part stemming from considering ideal mixing of different metallic phases.

To estimate the entropy of mixing S_{mix}, a non-interacting mixture was assumed (i.e. ideal mixing) and the initial step was to consider the Boltzmann-Planck equation from eq. (2.3)

$$S = k_{\text{B}} \log(\Omega) \,.$$

The possible microstates comes from basic combinatorics

$$\Omega = \frac{N!}{\prod_i N_i!} \,,$$

where N is the total number of atoms and N_i is the number of atoms of species i. Applying the logarithm and using Stirling's formula[1] [34, p. 374], yields

$$\begin{aligned} \log(\Omega) &= \log\left(N!\right) - \sum_i \log(N_i!) \\ &= \sum_i N_i(\log(N) - \log(N_i)) \\ &= -N \sum_i c_i \log(c_i) \,, \end{aligned} \tag{3.5}$$

with concentrations

$$c_i = \frac{N_i}{N} \,,$$

and the leading N before the sum disappearing when entropy per atom is considered.

Another consideration when changing to energy per atom (which we want to do) is that the original stochiometric formula changes

$$\frac{x}{x+2}\text{Me} + \frac{1}{x+2}\text{O}_2 \leftrightharpoons \frac{1}{x+2}\text{Me}_x\text{O}_2 \,,$$

note that there is now one atom in total on each side of the transition. This also means that

$$n_{\text{O}_2} = \frac{1}{x+2} \,,$$

note that this is actually half the ratio of oxygen atoms per atom in the metal oxide. In other words

$$n_{\text{O}_2} = \frac{r_{\text{O}}}{2} \,. \tag{3.6}$$

Finally, using the results obtained in eqs. (3.1) to (3.6) the Gibbs free energy of formation could be described as

$$G_{f,\text{Me}_x\text{O}_2}(T,p) = U_{f,\text{Me}_x\text{O}_2}(0\,\text{K}, 0\,\text{Pa}) - \frac{r_{\text{O}}}{2}\mu_{\text{O}_2} - TS_{\text{mix}} + \int_{0\,\text{K}}^{T} C_V^f(T')\,\text{d}T' \,,$$

[1] This is an approximation that can be used when N is large.

where

$$C_V^f(T) = \frac{1}{x+2} C_V^{\mathrm{Me}_x\mathrm{O}_2}(T) - \frac{x}{x+2} C_V^{\mathrm{Me}}(T)\,.$$

However, as C_V^f is not known from the DFT databases we will assume that the specific heat is the same for the metal and the metal oxide for the same amount of substance, i.e. $C_V^{f'}(T) - C_V^f(T) = 0$. To simplify a little bit further we will do a zeroth order Taylor expansion of the mixing entropy contribution around some reference temperature T_{ref},

$$G_{f,\mathrm{Me}_x\mathrm{O}_2}(T,p) = U_{f,\mathrm{Me}_x\mathrm{O}_2}(0\,\mathrm{K}, 0\,\mathrm{Pa}) - \frac{r_{\mathrm{O}}}{2}\mu_{\mathrm{O}_2} - T_{\mathrm{ref}} S_{\mathrm{mix}}\,.$$

We renormalise the energy and rewrite this as

$$\tilde{G}_{f,\mathrm{Me}_x\mathrm{O}_2}(\mu_{\mathrm{O}_2}) = \tilde{U}_{f,\mathrm{Me}_x\mathrm{O}_2} - \frac{r_{\mathrm{O}}}{2}\mu_{\mathrm{O}_2}\,. \tag{3.7}$$

Note that this is the equation of a straight line with intersect $\tilde{U}_{f,\mathrm{Me}_x\mathrm{O}_2} = U_{f,\mathrm{Me}_x\mathrm{O}_2} - T_{\mathrm{ref}} S_{\mathrm{mix}}$ and slope $-\frac{r_{\mathrm{O}}}{2}$.

3.4 Thermodynamically favoured phase transitions

To identify thermodynamically favoured phase transitions, first the stable phases at different conditions was found. This was done by finding the phase with lowest Gibbs free energy for some certain elemental composition, using the renormalised Gibbs free energy from eq. (3.7). Where we found that we can parameterisise the free energy in terms of the chemical potential of oxygen and write this as a straight line with

$$\begin{aligned} \tilde{G}_f(\mu_{\mathrm{O}_2}) &= m\mu_{\mathrm{O}_2} + b \quad \text{with} \\ b &= U_{f,\mathrm{Me}_x\mathrm{O}_2} - T_{\mathrm{ref}} S_{\mathrm{mix}} \quad \text{and} \\ m &= -\frac{r_{\mathrm{O}}}{2}\,. \end{aligned}$$

where the mixing contribution was approximated by fixing $T_{\mathrm{ref}} = 1200\,\mathrm{K}$. Note that this is the equation of a straight line with slope m and intersect b.

By identifying each compound with a straight line, the problem of finding the stable phase at some oxygen chemical potential μ_{O_2} could be solved by finding the convex hull in terms of oxygen content and free energy. When translated to $(\mu_{\mathrm{O}_2}, \tilde{G}_f)$-space this problem becomes instead the task of finding the lower bound for all energies, see fig. 3.2. Crossing lines signify a phase transition and phase transitions on the convex hull are the thermodynamically favoured phase transitions.

The term "convex hull", stems from geometry and is the smallest geometrically convex shape that contains the relevant set. As a matter of fact, the thermodynamically stable phases happen to lie on such a convex hull when considering the free energy [60–62] and is almost synonymous with finding the thermodynamically stable phases. Therefore, the term convex hull will be used synonymously with the thermodynamically stable phases even when the thermodynamically stable phases no longer form a convex hull due to choice of parameter space.

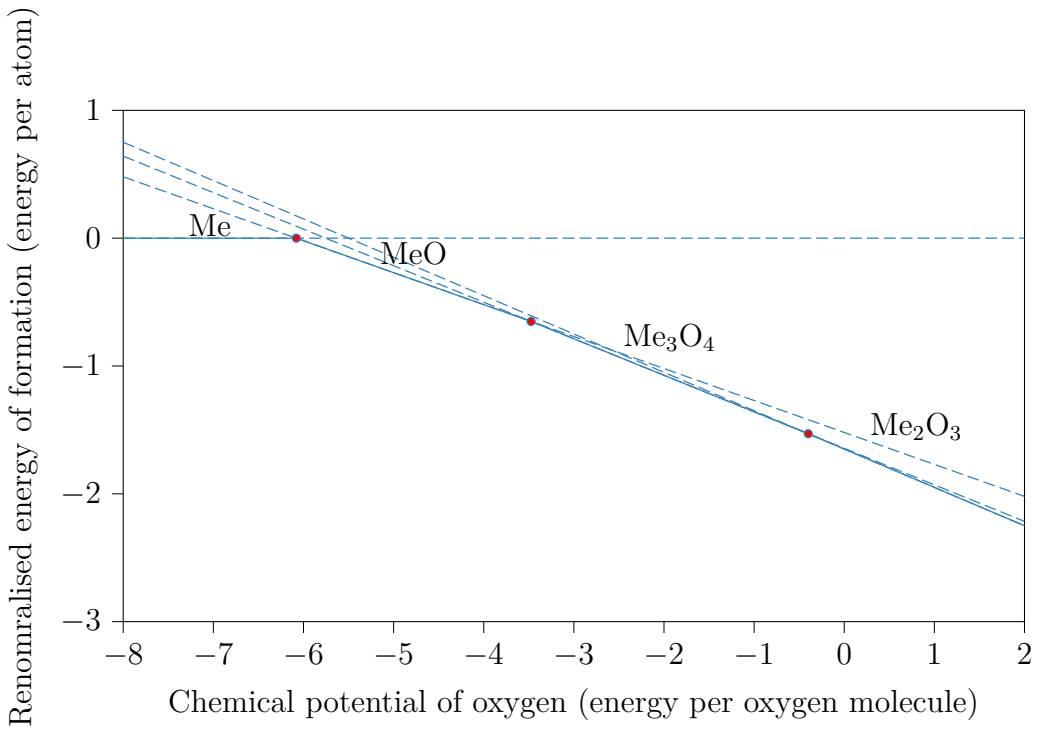

Figure 3.2: *Finding thermodynamically stable phase transitions. Each compund can be identified as a straight line and the currently stable phase is the line with the lowest renormalised Gibbs free energy of formation, $\tilde{G}_f$. Crossings of lines symbolises a phase transition. The currently stable phase is symbolised with a fully drawn line and the thermodynamically stable phase transitions are here marked by red dots.*

3.5 Chemical potential of oxygen

The usability of eq. (2.6) which describes the pressure dependence of the chemical potential, hinges on there being some values for $\mu_{O_2}(T, p_0)$ which can be calculated from eq. (2.7), given values for the enthalpy and the entropy of oxygen. These values for enthaply and enthropy where taken from the JANAF Thermochemical Table O-029 [50] (also [63, p. 1717]).

For values of temperature between the tabulated ones, an interpolated univariate spline of degree 3 and smoothing forced to 0 was used. This interpolation with the datapoints can be seen in fig. 3.3.

3.6 The modified Ellingham diagram

In the original unmodified Ellingham diagram the key quantity was Gibbs free energy of formation [64]. However, we will instead consider the modified Ellingham diagram where the key quantitiy is the Gibbs free energy of transition [14, 16, 29, 65] for the chemical reaction of a metal oxide going from reduced to oxidised phase

$$a\,\mathrm{Me}_x\mathrm{O}_y + \mathrm{O}_2 \rightleftharpoons a\,\mathrm{Me}_x\mathrm{O}_{(\mathrm{y}+2/\mathrm{a})}\,. \tag{3.8}$$

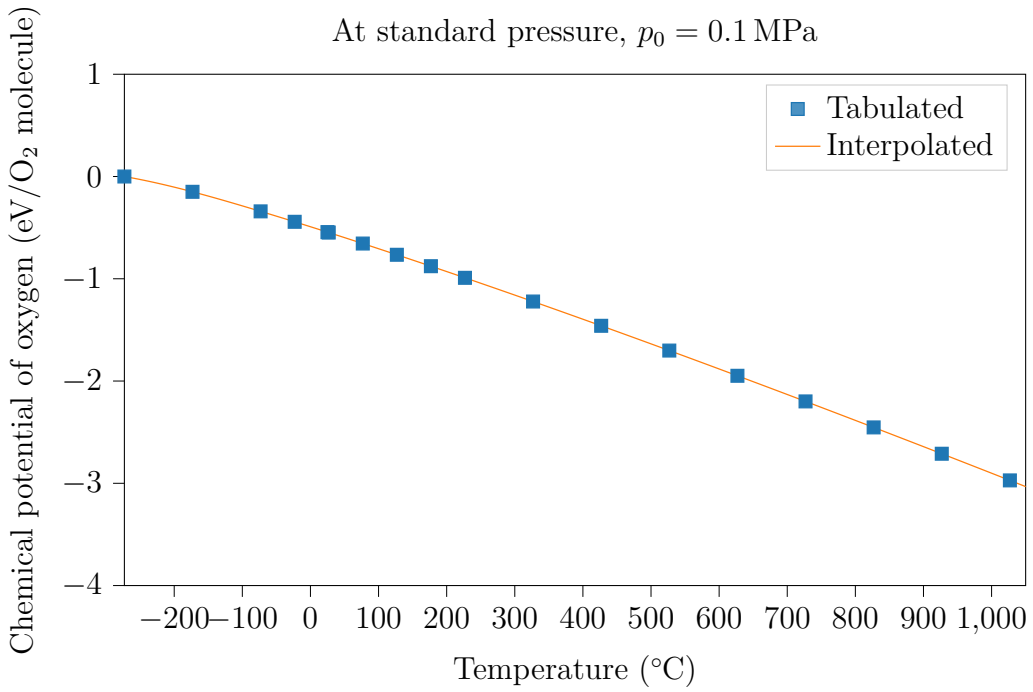

Figure 3.3: *The chemical potential of oxygen at* 0.1 MPa *and different temperatures. Both tabulated data from Linstrom and Mallard [50] as well as the interpolated line are shown.*

This is relevant for reactions that actually can occur. Therefore, we will only consider phase transitions between neighbouring phases on the same convex hull, see section 3.4.

For some transition as in eq. (3.8) we have a transition energy

$$G_t = aG_{\mathrm{Me}_x\mathrm{O}_{(y+2/a)}} - aG_{\mathrm{Me}_x\mathrm{O}_y} - (1\,\mathrm{O_2\,molecule}) \cdot \mu_{\mathrm{O_2}}\,,$$

which we can rewrite in a similar way as in eq. (3.7) to get

$$G_t = a(U_{f,\mathrm{Me}_x\mathrm{O}_{(y+2/a)}} - U_{f,\mathrm{Me}_x\mathrm{O}_y} - T(S_{\mathrm{mix},\mathrm{Me}_x\mathrm{O}_{(y+2/a)}} - S_{\mathrm{mix},\mathrm{Me}_x\mathrm{O}_y})) - \mu_{\mathrm{O_2}}(T,p)\,. \tag{3.9}$$

The sign of the transition energy in eq. (3.9) determines the direction of the chemical reaction in eq. (3.8), negative G_t and the oxidised phase is more stable than the reduced phase, and if positive vice versa. Remember that what we want is to find something that is reduced in the fuel chamber and oxidised in the air chamber. This is the same thing as finding a material that has a transition energy G_t that is negative in the conditions of the air chamber and positive in the conditions of the fuel chamber (note that for more complex CL processes than CLOU and CLC there might be some further considerations).

Furthermore, for some fixed temperature T we can translate the transition point where $G_t = 0$ into a value for the partial pressure of oxygen with the relation from eq. (2.6). Knowing at which partial pressure of oxygen this transition occurs is enough to determine whether an OC can work in CLOU. However for other CL

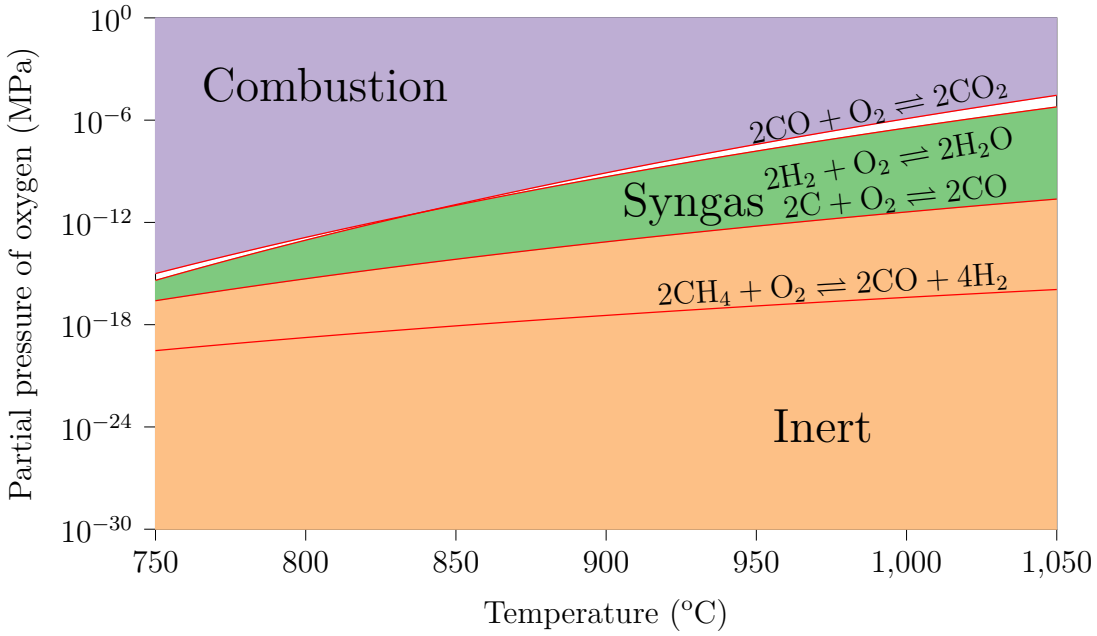

Figure 3.4: *Regions for different CL processes in the modified Ellingham diagram. The red lines correspond to equilibria for different transitions. Adapted from Fan, Zeng, and Luo [29].*

processes it is usually necessary to take attributes of the fuel into consideration. In fig. 3.4 regions for two different CL processes are illustrated as adapted from [29], see the original work for details. However, when direct interaction with fuel is necessary kinetics of the reactions might become important and furthermore, special consideration will have to be taken for each fuel. Therefore, this work will be limited to finding materials for CLOU.

3.7 Mixing metals – a recipe for alloys

The natural extension of considering a metal oxide with a single metal is to consider a metal oxide alloy with more than one metal. However, the first complication that arises is what ratios between the different metals to consider. There are at least two simple ways to resolve this.

The first one to consider is an evenly spaced mesh in the composition space, e.g. for an alloy A_xB_y with $(x, y) \in \{(1, 0), (0.9, 0.1), (0.8, 0.2), \ldots, (0, 1)\}$. However, an evenly spaced mesh is not always natural for all alloys. Oftentimes a ratio between elements could possibly yield nothing but binary mixtures and not a pure alloy anywhere on the convex hull, as the ratios are not exactly correct.

The second method is a way to mitigate this problem. If one considers all metal ratios that exist in the database for some set of metals then these ratios at least have a possibility of having pure alloys in their convex hull. In this thesis the second method is the primary method that will be used to investigate mixes of metals as candidates for metal oxides.

When one has determined the ratio between metals in a mixture the next step is

finding possible mixes alloys and pure metals. First off, given some ratio of metals

$$\vec{r_0} = \begin{bmatrix} r_{0,1} & r_{0,2} & r_{0,3} & \vdots & r_{0,n} \end{bmatrix},$$

then a mix that is possible fulfils the equation

$$\begin{bmatrix} r_{0,1} & r_{0,2} & r_{0,3} & \dots & r_{0,n} \end{bmatrix} = \begin{bmatrix} c_1 & c_2 & c_3 & \dots & c_m \end{bmatrix} \begin{bmatrix} r_{1,1} & r_{1,2} & r_{1,3} & \dots & r_{1,n} \\ r_{2,1} & r_{2,2} & r_{2,3} & \dots & r_{2,n} \\ r_{3,1} & r_{3,2} & r_{3,3} & \dots & r_{3,n} \\ \vdots & \vdots & \vdots & \ddots & \vdots & \vdots \\ r_{m,1} & r_{m,2} & r_{m,3} & \dots & r_{m,n} \end{bmatrix},$$

$$\begin{bmatrix} \vec{r_0} \end{bmatrix} = \vec{c} \begin{bmatrix} R \end{bmatrix},$$

where elements in $\vec{c}$ are the coefficient before each separete phase in the mix of phases. For example, when considering if Fe_2O_3 and TiO_2 can be a possible phase for an equal mixture of Fe : Ti, we have

$$\begin{bmatrix} 1, 1 \end{bmatrix} = \vec{c} \begin{bmatrix} 2, 0 \\ 0, 1 \end{bmatrix},$$

with solution

$$\vec{c} = \begin{bmatrix} 0.5, 1 \end{bmatrix}.$$

Note that the oxygen is not considered when balancing the formula as the oxygen content can change in the considered chemical reaction.

Furthermore, note that if the matrix on the right hand side has linearly dependent rows there are infinite solutions to find $\vec{c}$. This may seem problematic. To resolve of this problem, remember that the goal is still to find the convex hull eventually and that only one phase is stable at some temperature and pressure (exept exactly when the phase transitions is in equilibrium), as such, it suffices to find all solutions where the rows are linearly independent.

To find these linearly independent solutions the idea is to try all combinations of compounds to build a matrix R of vectors $\vec{r_i}$ that have no more rows than the number of elements in the space to search, i.e. the number of (nonzero) entries in the vector $\vec{r_0}$. Furthermore this matrix should have full rank. Only when these criteria are fulfilled, we will check whether there exist a solution with positive values in $\vec{c}$.

3.8 Overview of code base

In handling the code an object oriented programming framework was adapted and a few different classes and objects were created.

The information in a chemical compound (e.g. Fe_2O_3 or $FeTiO_3$) were saved as an instance of a class Compound. Combination of compounds (e.g. $xFe_2O_3 + yFeTiO_3$) is considered a Phase instance and collection of Phase instances with the same ratio of metallic species was in turn called a Phases instance. This Phases class had in turn a subclass ConvexHull which is the Phases that are thermodynamically stable. All these objects were handled with a class called ThermoData that could create instances of the previously mentioned classes from data on the OQMD.

3.8.1 Finding stable phase transitions

The first step that was considered was how to determine which ratios of elements to consider. For monometallic compounds all phases were considered. However, when considering bimetallic or trimetallic phases only ratios in the database that existed as an entry were considered primarily. Though if preferred, any ratio of metals is possible.

Considering the possible phases (see section 3.7) then the convex hull was found as in section 3.4. This convex hull consist of the stable phases.

3.8.2 Modified Ellingham diagram

When using the modified Ellingham diagram for finding relevant materials for CL processes, many processes are fuel dependent. As such, this project made a limitation in finding CLOU materials as this is not fuel dependent as long as the fuel can react with free oxygen.

Even when limited to CLOU there is a question of, for which values of temperatures and partial oxygen pressures the relevant phase transition should take place. These values were determined in collaboration with people from the *Department of Space, Earth and Environment*[2] as well as from the *Department of Chemistry and Chemical Engineering*[3] at Chalmers University of Technology.

The phase transition should happen in the temperature span of 750 °C to 1050 °C. The motivation for the temperature is that this is around standard operating temperature for the type of fluidised bed reactor that is used in CLC. As for the partial oxygen pressure it was set to a single limit of 5 kPa. If the OC oxidises above 5 kPa (i.e. 5 % oxygen in a gas mix of about the standard atmospheric pressure) then it oxidises in the air chamber even if the oxygen content has gone down somewhat. Similarily, in the fuel chamber the fuel will react with any available oxygen and keep the oxygen content in the surrounding gas well below 5 kPa, i.e. the OC releases oxygen (is reduced) in the fuel chamber. This criteria as marked on an empty ellingham diagram is illustrated in fig. 3.5.

3.9 Filtering materials

While the main consideration has been to find what materials could work in the CLOU process, there are other considerations. Some materials are radioactive, toxic or otherwise harmful either to people or the environment [66] and these are not materials which are wanted. Other could come from conflict minerals from mines that wars are being fought over [67] and could be excluded from ethical considerations. Others do not exist naturally or only exist as part of a decay chain [68]. Beyond these consideration, price may also play some role into which compounds that are relevant [69]. In fig. 3.6 some of these considerations are illustrated with a periodic table.

[2]Tobias Mattisson, Yongliang (Harry) Yan and Arijit Biswas
[3]Henrik Leion and Rizwan Raza

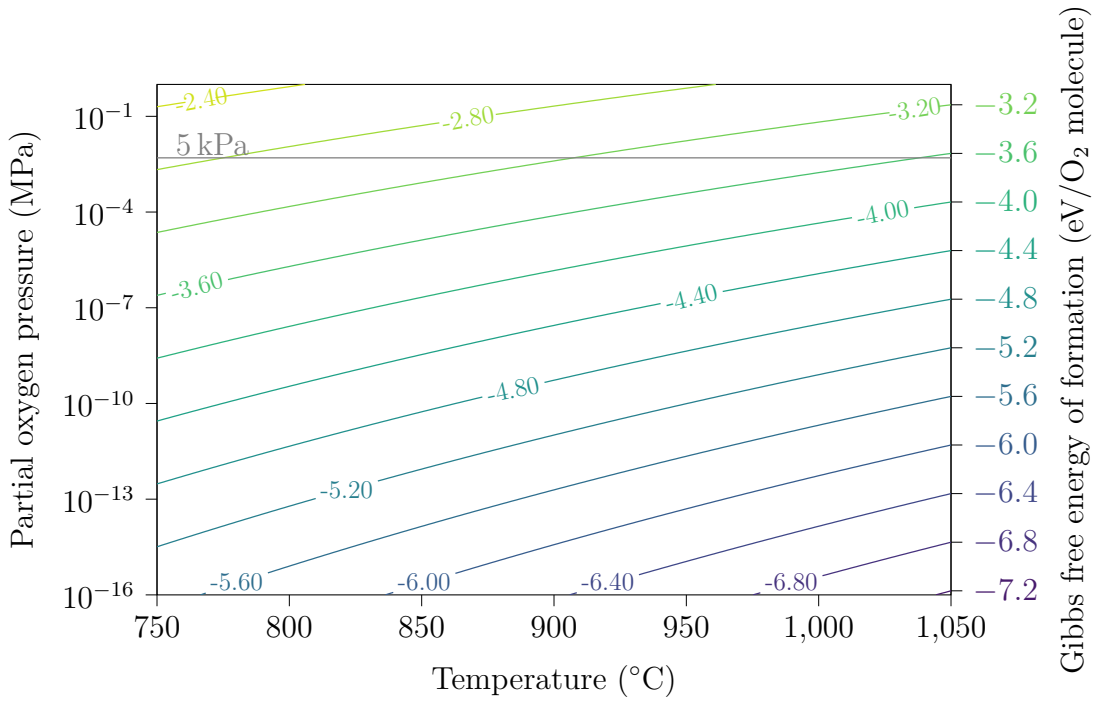

Figure 3.5: *Correspondence between partial pressure of oxygen and Gibbs free energy of formation. The criteria for CLOU materials is the grey horisontal line at* 5 kPa *partial pressure of oxygen. The equilibrium between oxidation and reduction of the OC should cross this line in the temperature region* 750 °C *to* 1050 °C.

Furthermore, the physical stability of the metal oxide filaments that are used in CLOU should have a durability that lasts several cycles. While the durability is hard to estimate when considering thermodynamics of perfect bulk crystals, the melting point can be estimated from other sources [70].

The above mentioned practical considerations can be used as a filter to determine which materials should be used in screening. In table 3.1 the result of different steps of this filtering is shown. When using these filters 27 elements remain in the end, however the last two filters will be applied on each specific transition and therefore 51 elements will be considered initially for polymetallic systems.

Note, that these filters have been applied on the elemental phases in this case, the oxidised phases or alloys with several elements could have other specifics for toxicity, hasardousness, price and melting point. The ones that are expected to vary especially much compared to the elemental phase are price and melting point.

For alloys the price and melting point have been averaged over the composition of elements. Therefore these last two filters will be applied for each composition rather than on the composing elements. Furthermore, generous values have been used as threshold in the filters for price (1000 \$/kg) and melting point (900 K), as these are quite uncertain estimates of the true values.

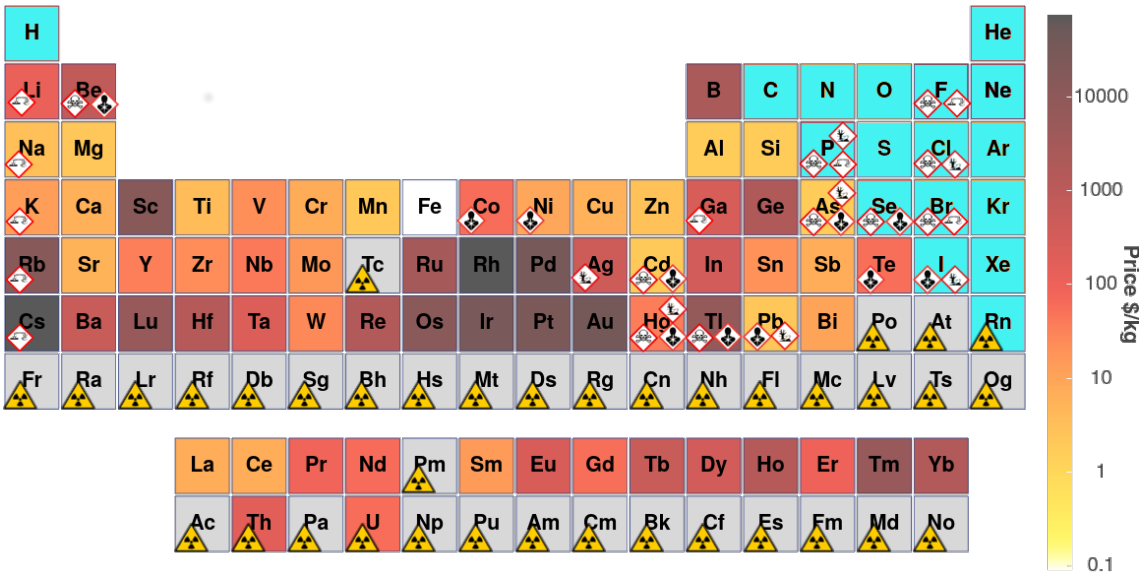

Figure 3.6: *Periodic table color-coded after price. Nonmetals are colored light blue and those with unknown price are grey. Hazard symbols connected to the bulk state of the elements are added to this. Note that Fe has a white background simply because it is so cheap.*

3.10 Ranking the CLOU candidates

There have been a few different criteria mentioned previously in the thesis. However, to be able to rank the potential OCs that remain after filtering on practical aspects, a single quantitative measure is needed. The best measure for this is the cost the OC adds to the cost of capturing carbon dioxide. In other words, cost per mass of carbon dioxide captured [71]

$$\mathrm{CCC_{OC}} = \frac{C_{\mathrm{OC}} \cdot \mathrm{SI}}{\mathrm{SE} \cdot \eta_{\mathrm{CO_2}} \cdot \tau},$$

where C_{OC} is the cost of OC per mass unit and τ is the life time of the oxygen carrier. The remaining part comes from the mass of oxygen carrier per power unit produced ($\propto$ SI, SI stands for solid inventory) and the amount of carbon dioxide released per energy produced ($\propto \mathrm{SE} \cdot \eta_{\mathrm{O_2}}$, SE stands for specific emission). While some of these parameters are fuel and boiler dependent it is possible to establish something that should be approximately capture the idea behind the oxygen carrier carbon capture cost $\mathrm{CCC_{OC}}$.

First off, consider our criteria for what constitutes a CLOU OC: The material should have a transition that is in equilibrium somewhere in the temperature range 750 °C to 1050 °C, at an oxygen partial pressure of 5 kPa. However the estimated transition energy that lays the foundation for this has some uncertainty. As such, instead of having candidates that either are CLOU materials or not, we have evidence for some specific credence that a material is a CLOU OC. This is illustrated in fig. 3.7. A qualitative measure has been explored, however for the score the credence

Table 3.1: *When applying different filters the available metals are reduced. The first filter is applied on all elements and the other filters are applied only on metallic elements.* Set *indicates the size of the set on which the filter is applied,* Removed *are how many of those that were removed by the filter and* Remaining *are the number of elements that remain after the filter. The sequential adding of filters will be carried out to reduce the search space to more relevant materials.*

Filter layer	Only one filter			Sequantially added		
	Set	Removed	Remaining	Set	Removed	Remaining
All metals	118	17	101	118	17	101
Not synthetic	101	24	77	101	24	77
Not from decay	101	8	93	77	8	69
Not conflict	101	4	97	69	4	65
Not toxic	101	4	97	65	4	61
Not radioactive	101	36	65	61	5	56
Not hasardous	101	8	93	56	5	51
Max price: 1000 \$/kg	101	53	48	51	17	34
Min melting point: 900 K	101	39	62	34	7	27

for the energies were simply a Gaussian distribution around the estimated energy with standard deviation $1\,\mathrm{eV}/\mathrm{O}_2$ molecule.

The way to calculate this credence of being an OC for CLOU is to calculate the probability that the equilibrium line in the modified Ellingham diagram is above or below the 5 kPa line. One way to calculate this is to estimate the credence that the equilibrium for the phase transition is below (or above) 5 kPa at 750 °C and on the opposite side of 5 kPa at 1050 °C. In other words

$$\mathrm{P}(\text{OC for CLOU}) = \sum_{i=\left\{\substack{\text{above,}\\\text{below}}\right\}} \mathrm{P}(i|T = 750\,^\circ\mathrm{C}) \cdot \Big(1 - \mathrm{P}(i|T = 1050\,^\circ\mathrm{C})\Big)\,,$$

here it is assumed that the equilibrium line is continuous and that the unceratinty in energies are uncorrelated at 750 °C and 1050 °C.

The second thing to consider is how much carbon dioxide a certain mass of OC produces before it has to be replaced. This is related to how much fuel an OC can combust and should therefore be high. The amount of carbon dioxide produced is directly related to how much oxygen the OC can transport between the chambers. With lack of any better estimate a flat credence of the lifetime τ of an oxygen carrier will be used, i.e. in practice we will assume that all oxygen can survive the same amounts of loops on average through the CLOU reactor chambers. With this assumption the oxygen transport capacity OTC is defined as the mass ratio of oxygen transported per loop is proportional to the mass carbon dioxide produced

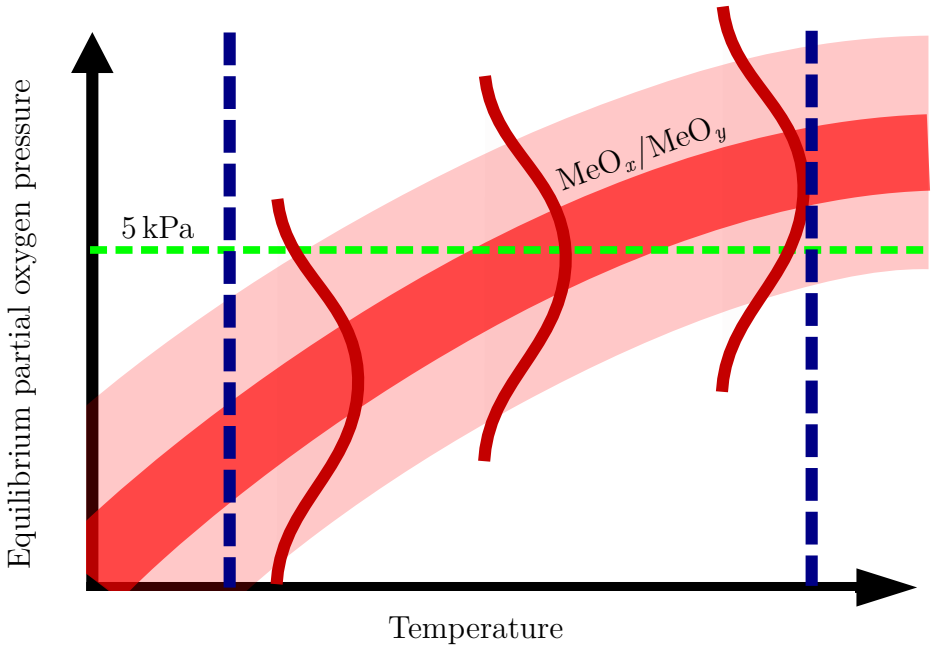

Figure 3.7: *The uncertainty in energy (red regions) leads to an uncertainty along the y-axis in the modified Ellingham diagram. This implies that there also is an uncertainty in exactly where the line crosses the equilibrium partial pressure criteria of* 5 kPa *(horizontal dashed green line). Which in terms leads to a probability that the crossing is within some temperature region (vertical dashed blue lines).*

per mass of oxygen carrier used. In other words

$$\mathrm{OTC} = \frac{m_{\mathrm{O_2}}}{a m_{\mathrm{Me_xO_{(y+2/a)}}}},$$

or equivalently

$$\mathrm{OTC} = \frac{m_{\mathrm{Me_xO_{(y+2/a)}}} - m_{\mathrm{Me_xO_y}}}{m_{\mathrm{Me_xO_{(y+2/a)}}}},$$

where m_{X} is the mass of the corresponding phase in eq. (3.8).

The third and last criteria to consider is simply the estimated price per mass unit of OC. However something that is twice as expansive is half as good. At least when with respect to $\mathrm{CCC}_{\mathrm{OC}}^{-1}$ and assuming equal life times. Therefore, the quantity that is proportional to the reciprocal of $\mathrm{CCC}_{\mathrm{OC}}$ is mass of OC per amount of currency.

Using these three quantifiers a formula for a score can be established

$$\mathrm{Score} = 100 \cdot \mathrm{P(OC\ for\ CLOU)} \cdot \mathrm{OTC} \cdot \frac{50\,\$/\mathrm{kg}}{C_{\mathrm{OC}}}.$$

The factor 100 and the factor 50 \$/kg is purely so that the score, Score, is unitless and of a reasonable size. This way something hypotethical that is an OC for CLOU with probability one, has an oxygen transfer capacity $\mathrm{OTC} = 1$ and costs $C_{\mathrm{OC}} = 50\,\$/\mathrm{kg}$, has a score: $\mathrm{Score} = 100$.

3.11 Validating results

To know if the results could be used for anything they had to be validated in some way. Two approaches were used. One where the implications for some of the approximations in the theory are investigated with some more exact theory. And another one where the results are compared to values from experimental methods.

3.11.1 Contributions from phonon corrections

The correction for the phonon contribution was calculated using the small displacement method as implemented in Atomic Simulation Environment (ASE) [72]. The calculator that was used was the Vienna Ab initio Simulation Package (Vasp) [73–76] with the projected augmented wave method [77, 78] and generalised gradient approximation PBE exchange correlation functional [42, 79].

These calculations were done for Fe and FeO. To find values for parameters such as plane wave cutoff, size of supercell and number of k-points, the potential energies were converged to around 1 % (i.e. ∼10 meV). This meant an energy cutoff of 600 eV, a supercell with three primitive cells in each direction and 5 k-points in each direction. Other parameters that were used were either default from the Vasp interface in ASE or as stated in table 3.2.

Table 3.2: *Parameters for phonon calculations as sent to the Vasp interface in ASE.*

Param.	prec	xc	algo	encut	sigma	ispin	kpts	lplane	lreal
Value	Normal	PBE	Fast	600	0.05	2	5	True	Auto

3.11.2 Comparing with experimental data

Experimental data from Linstrom and Mallard [50] and the Shomate equation from section 2.5 were used to estimate the Gibbs free energy of transition for some monometallic transitions. Furthermore, data from Pröll [65] (whose data were in turn from the HSC Chemistry 6.1 software with corresponding database) were also used.

Chapter 4

Results

When searching for OCs for CLOU a lot of different combinations of materials where considered and many potential OCs where also found. All the transitions will not be presented but a numerical summary can be found in section 4.1.

Further findings include a few different methodologies to find the associated phase diagrams for all the entries in the database. A method for constructing the modified Ellingham diagram has been constructed, which is a key method for investigating OCs thermodynamically. The top candidates for OCs in the CLOU process is presented and finally the validity of the results is examined.

4.1 Numerical summary of considered elements

The summary in table 4.1, concerns five different subsets of all combinations of compounds in the OQMD. The first two subsets are for all monometallic ($n = 1$), and mono- and bimetallic ($n = 1$) compounds in the database. The other three subsets are for filtered materials. They were filtered as described in section 3.9 and $n = 3$ denotes that mono-, bi- and trimetallic compound and combinations were considered.

Table 4.1: *Summary of all the transitions that have been found to have potential to be good for CLOU. The space columns simply denotes whether the search space was filtered or not, as well as the highest number of elements allowed in a single compound. See text for a detailed description.*

Space	Elements considered	Combinations	Convex hulls	Stable phase transitions	Potential CLOU materials
All $n = 1$	100	100	73	150	8
All $n = 2$	100	5050	19 989	91 607	4433
Filtered $n = 1$	27	27	27	57	0
Filtered $n = 2$	51	1326	3601	18 193	452
Filtered $n = 3$	51	22 151	33 999	253 623	6538

The filtering is most apparent in the column denoted *Elements considered*. These

denote the number of elements in the periodic table that were considered, 100 corresponds to all metallic compounds in the periodic table, 23 the number of elements that pass all filters as described in table 3.1 and 51 the remaining elements when all filters except price and melting point were applied. The reason that the price and melting point filteres does not show up in this column for polymetallic compounds, is that these were applied on a compound basis. An example to illustrate this is that if a compound A is too expensive but a compound B is not too expensive, then AB might still pass the filter even though A would not pass the filter. For all filters beside those based on price and melting point, all elements in a compound must pass the filter for the whole compound to be able to pass the filter.

Combinations are simply the number possible combinations of when combining the considered elements and a maximum number of elements n in a combination.

Convex hulls are when things start getting interesting. These are the number of unique metal ratios that have two or more stable phase transitions. In other words, these are the numbers of possible materials for which at least one phase transition between stable phases have been found. *Stable phase transitions* are similarily, when all phase transitions on a convex hull are counted.

Finally, *Potential CLOU materials* are the number of convex hulls that have at least one phase transition whose equilibrium temperature is in the range 750 °C to 1050 °C when the partial oxygen pressure is 5 kPa. Which is actually the number of materials that have been found to be thermodynamically favoured for being OCs for CLOU.

4.2 Finding stable phase transitions

In the process of finding the possible CLOU materials, a step on the way was to find the stable phase transitions. This can be equated to finding the phase diagrams, which is a way to visualise the stable phases. All the phase diagrams in this section has been found through the method described in section 3.4.

When finding the stable phases we have primarily considered the chemical potential of oxygen and the Gibbs free energy. Therefore, it is natural to construct a phase diagram in that parameter space. Such a phase diagram for iron is visualised in fig. 4.1. In the phase diagram each phase corresponds to a dashed line and the currently stable phase is fully drawn. Note how the connected straight line "contains" all other lines, this is why the stable phases are called the *convex hull*. Furthermore, the thermodynamically favoured phase transitions are the points where the lines connect with each other on the convex hull.

Note how the least oxidised phase Fe, show up furthest to the left and more oxidised phases all show incrementally to the right for larger values of the chemical potential. An interpretation of this behaviour is based on the chemical potential of oxygen, which is the change in free energy when adding a single oxygen molecule. Therefore, oxygen in gas phase is more preferable for negative values of the chemical potential as this would add an oxygen molecule to the system.

The convex hull can of course be drawn for each considered element and combination of elements. In fig. 4.2, the convex hulls are drawn for all of the monometallic

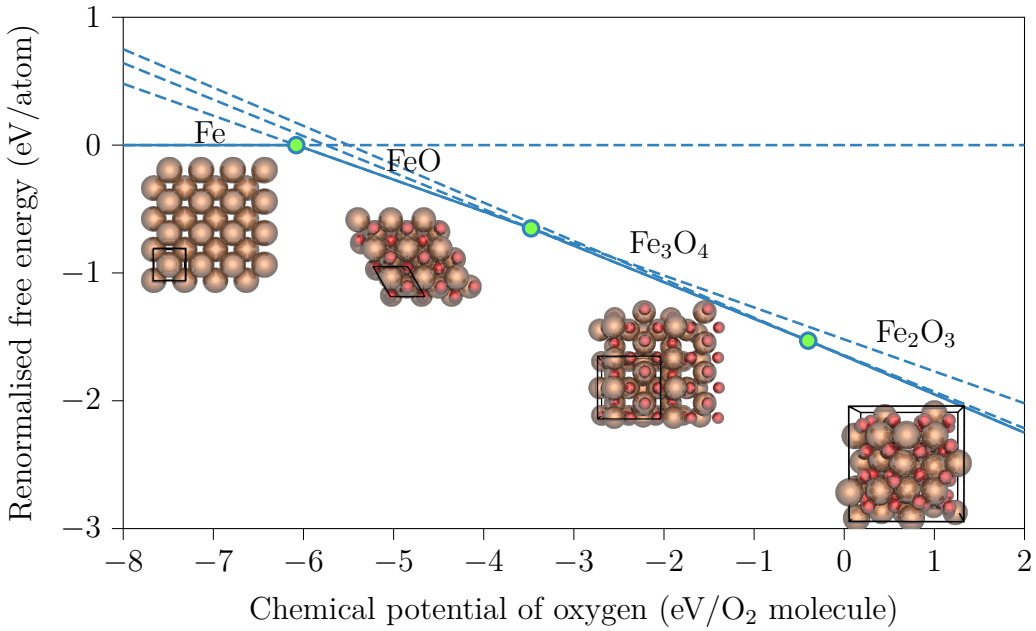

Figure 4.1: *Visualising a single convex hull, here iron was chosen as an example. The fully drawn lines is the convex hull with transitions at the points. The dashed lines are continuations of each phase, note that these are by definition never below the convex hull. Also added are the crystal structures of each material, the black lines indicate the unit cell.*

compounds that have passed the filters described in section 3.9. The restriction was made in attempt to keep the figure less cluttered.

As the Gibbs free energy has been renormalised for these different compounds with different renormalisation. One has to be cautions when comparing them to each other. However, there is still some physical behaviour that can be interpreted. Note the different compounds oxygen content at different values for the chemical potential of oxygen. Especially, note how the noble metal silver has very low oxygen content and is in its bulk phase of pure silver at an oxygen chemical potential of around $-1\,\mathrm{eV/O_2}$ molecule, while e.g. titanium, which is strongly coupled with oxygen, is oxidised even at very low values for the chemical potential of oxygen.

Furthermore, there is no need to be limited to monometallic compounds. Differences in composition space have also been considered. As an example the phase diagram for different ratios of iron and titanium against the chemical potential of oxygen can be found in fig. 4.3. When considering different mixes of only two elements, we can already see that things become more complicated. Also note, that all areas consist of a mix of two compounds. This is because each infinitesimal vertical slice consists of only a single ratio of iron against titanium and such a thin slice is the only place where a pure phase would be observed. Boundaries between filled areas are where phases are in equilibrium.

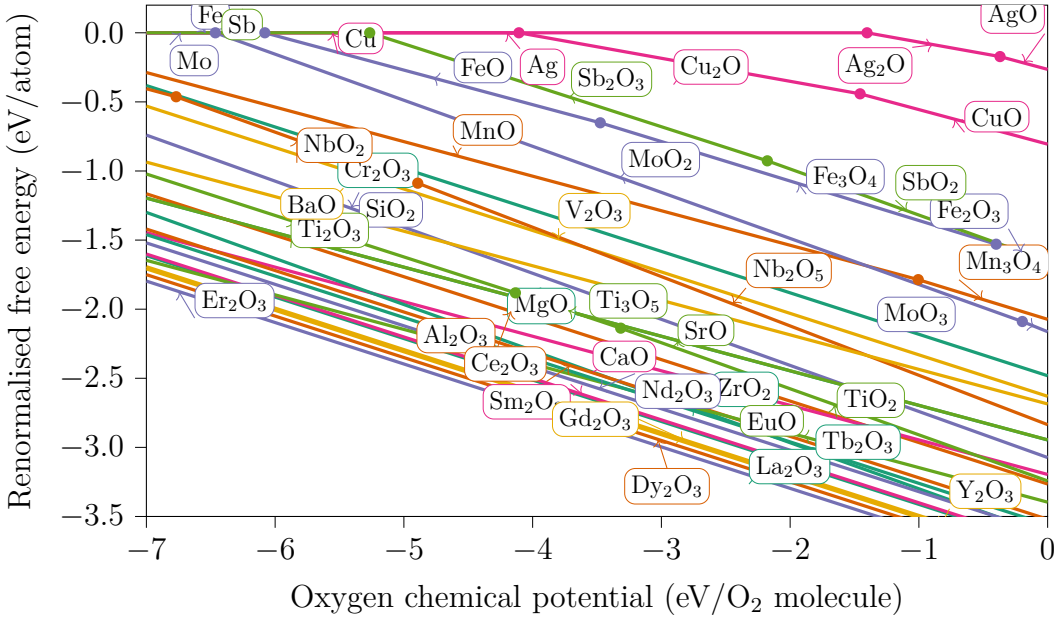

Figure 4.2: *Convex hulls for filtered monometallic OCs, i.e. nontoxic etc. The straight lines between points signify a stable phase, which is annotated. The points are the phase transitions.*

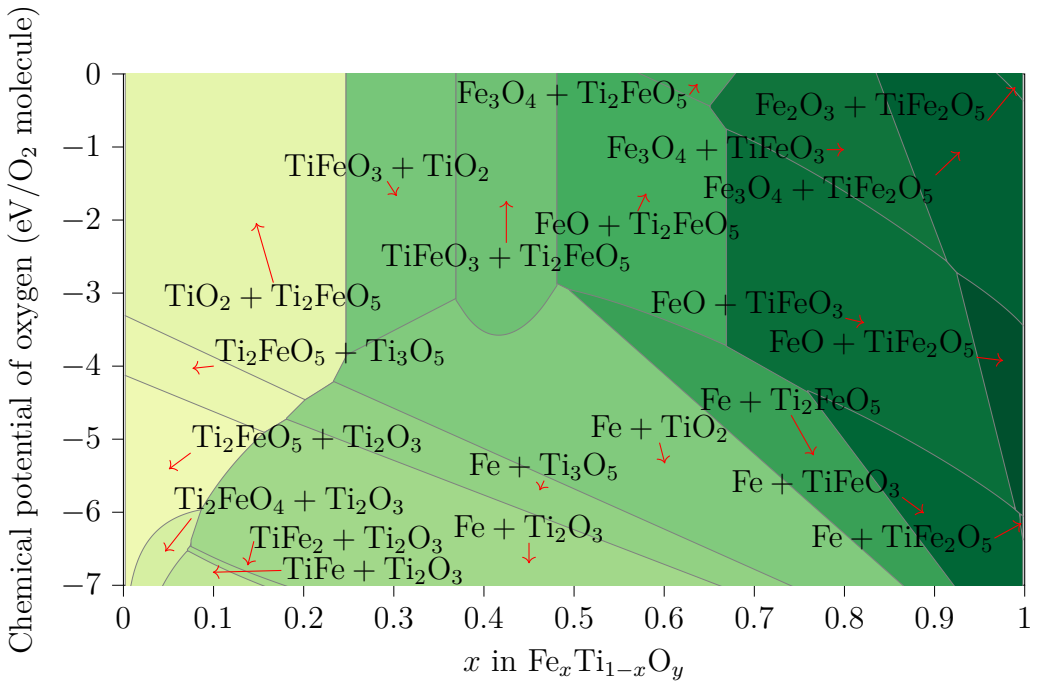

Figure 4.3: *The stable phase for ratios of iron in a mix of iron and titanium with chemical potential of oxygen on the y-axis. Note that the phases are not balanced and the plus sign only signifies that both phases appear.*

4.3 The modified Ellingham diagram

The modified Ellingham diagram is a way to visualise what materials that can work in different CL processes (including CLOU). Therefore, the possibility to generate this kind of diagram is important. This can be generated by finding the thermodynamically favoured phase transitions (section 4.2), translating the chemical potential of oxygen into partial pressure of oxygen and temperature and applying the methodology described in section 3.6.

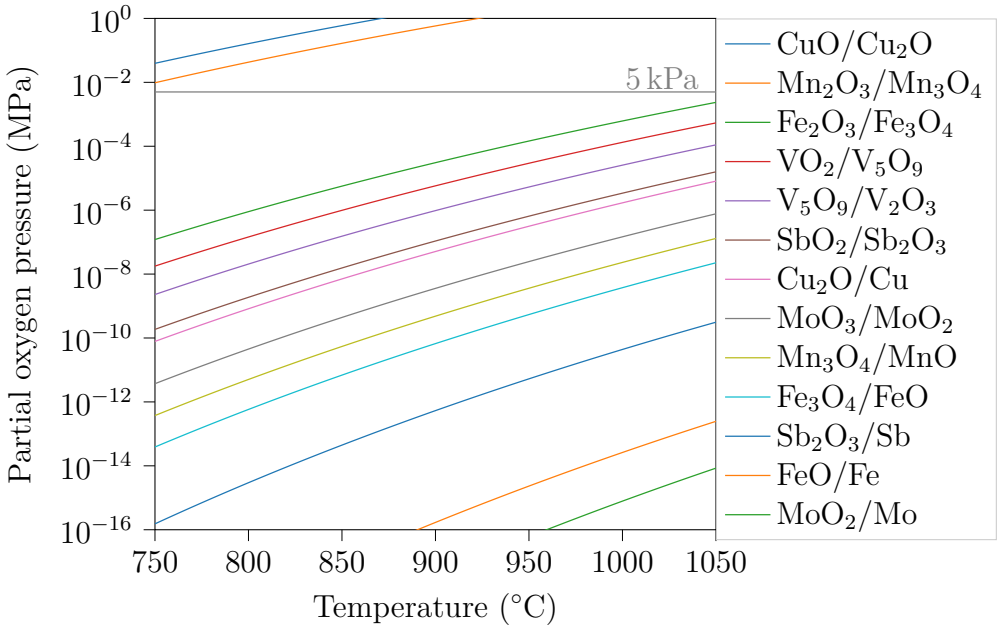

Figure 4.4: *The modified Ellingham diagram in the relevant region for filtered monometallic compounds. The horisontal grey line is the* 5 kPa *criteria for the equilibrium partial pressure of oxygen chosen for identifying OCs for CLOU.*

In fig. 4.4 the modified Ellingham diagram for the filtered monometallic compounds is shown. Note that in this diagram there is actually no line crossing 5 kPa partial pressure of oxygen. Thish means that there is no identified CLOU materials in the set of filtered monometallic compounds as seen earlier in table 4.1. In practice this does not actually mean that none of these materials could work for CLOU as the 5 kPa partial pressure of oxygen line crossing criteria is not actually a hard limit, transitions close to this line would still work. Furthermore, there is some uncertainty in these values and some materials could form oxygen vacancies and releasing oxygen without undergoing a full phase transition.

However, this indicates that it is not sufficient to investigate compounds with a single metallic element. Furthermore, we already know that the possible combinations of elements grows a lot when considering more and more elements. Therefore, a method for reducing the search space and prioritising this search is important.

4.4 Ranking the oxygen carriers

To be able to prioritise which materials to investigate a ranking system was developed. This ranking system was based on a score that is approximately proportional to mass of carbon dioxide produced captured per cost of OC material. It is in fact proportional to three different criteria, the probability that the transition in question would work in CLOU, the reciprocal of the material cost and the oxygen transfer capacity which is the amount of oxygen transferred from the air chamber to the fuel chamber per mass of OC and loop in the system. More details of how the score is calculated can be found in section 3.10.

Table 4.2: *The five most probable transitions for filtered mono-, bi- and trimetallic compounds.*

Place	Transition	Probability of crossing
1st	$\frac{552}{5}La_2O_3 + 96Mn_2BiO_5 + \frac{144}{5}MnBi_{12}O_{20} + O_2 \leftrightharpoons \frac{322}{5}La_2O_3 + \frac{184}{5}MnBi_{12}O_{20} + 92LaMn_2O_5$	0.995
2nd	$\frac{330}{13}Fe_2O_3 + \frac{180}{13}FeSb_2O_6 + \frac{120}{13}Li_4FeSbO_6 + O_2 \leftrightharpoons \frac{32}{13}LiFe_5O_8 + \frac{128}{13}FeSb_2O_6 + \frac{224}{13}Li_2Fe_3SbO_8$	0.815
3rd	$16Tb_2O_3 + 24Li_3VO_4 + 8Li_7VO_6 + O_2 \leftrightharpoons 14Tb_2O_3 + 4Li_8TbO_6 + 32Li_3VO_4$	0.795
4th	$16Y_2O_3 + 24Li_3VO_4 + 8Li_7VO_6 + O_2 \leftrightharpoons 14Y_2O_3 + 32Li_3VO_4 + 4Li_8YO_6$	0.779
5th	$16Dy_2O_3 + 24Li_3VO_4 + 8Li_7VO_6 + O_2 \leftrightharpoons 14Dy_2O_3 + 4Li_8DyO_6 + 32Li_3VO_4$	0.772

However, before considering the ranking according to the score parameter we can see what transitions are the most probable ones. The five most probable CLOU transitions when considering mono-, bi- and trimetallic compounds are listed in table 4.2.

Note that none of these transitions are transitions that where especially expected to show up beforehand. Rather, the reason that these show up as well as the reason that all are combinations with three elements are probably due to shear amount of extra compositions that appear when considering mixes of several elements. This would be a case in favour for having a fast high-throughput screening methodology as this facilitates a larger search space within reasonable time.

Furthermore, the probability of crossing has not gone above 80 % for all but two of the over 250 000 stable phase transitions. This is probably due to the relatively high uncertainty in the chosen distribution of credence (1 eV/O_2 molecule). Therefore, it could be worthwhile to try and increase this accuracy of the methodology and at the very least to determine the accuracy more exactly. The accuracy is further investigated and explored in section 4.5.

Knowing the most probable transitions, perhaps even more interesting are the ones with the best score, i.e. the ones that have the highest expected usefulness. In table 4.3 the top 10 highest ranked transitions for all filtered mono-, bi- and trimetallic phases are included. The very best score was achieved by the hematite to magnetite transition,

$$4Fe_3O_4 + O_2 \leftrightharpoons 6Fe_2O_3\,,$$

with a score of 443, which is an order of magnitude higher than the closest (non-iron) competitors. However, the main reason for this high score is that iron is at least two orders of magnitude cheaper than almost any other material. Therefore, even though the hematite to magnetite transition only has a probability of 48 % of crossing the 5 kPa partial oxygen pressure line in the temperature range 750 °C to 1050 °C, it still retains a high score.

Other observations of note is that sodium shows up on the list alloyed to some other metallic elements. Sodium is a cheap element and light and as such would have a high oxygen transfer capacity. However, sodium has a melting below 900 K and is therefore filtered away when considering monometallic compounds. Experiments would have to determine whether any of these materials actually work for CLOU and if their durability high enough.

It may seem that the probability of crossing is not such an important parameter. However, while not instantly apparent from these reduced ranking lists, note that the chosen distribution of credence (i.e. the probability distribtution) was a Gaussian distribution and that results several standard deviations away quickly become very small. This is more apperent in the more complete rankings in appendix A. Therefore this criteria has significantly reduced the chances for some compounds to appear high in the rankings.

For those interested longer and more diverse ranking lists have been compiled in appendix A.

4.5 Validation of methodology

To know whether the simplifications made in the extrapolation from 0 K were reasonable, a comparison to other, presumably more exact methods, has been made. This is important for primarily one aspect. Whether this methodology could be used at all or if other computationally more expensive methods or experiments would have to be used.

Comparing transition energies with values from experiments and the size of the neglected phonon contributions can be seen in table 4.4. The number of compared transitions are not enough to get more than a qualitative overview of how the different methods compare. However, from the mean differences it seems that a consequence of neglecting temperature dependence is that the transition energies are somewhat underestimated (in the absolute sense). This can be seen when comparing with e.g. JANAF [63] and the Shomate equation (see section 2.5). At 750 °C the energy difference is on average 0.48 eV/O_2 molecule and at 1050 °C the energy difference is on average 0.64 eV/O_2 molecule.

Note that for the theoretical values as derived in this thesis are constant as most of the temperature dependence is neglected. That the errors in table 4.4 increase for larger temperatures is precisely because the theoretical values neglect most of the temperature dependence.

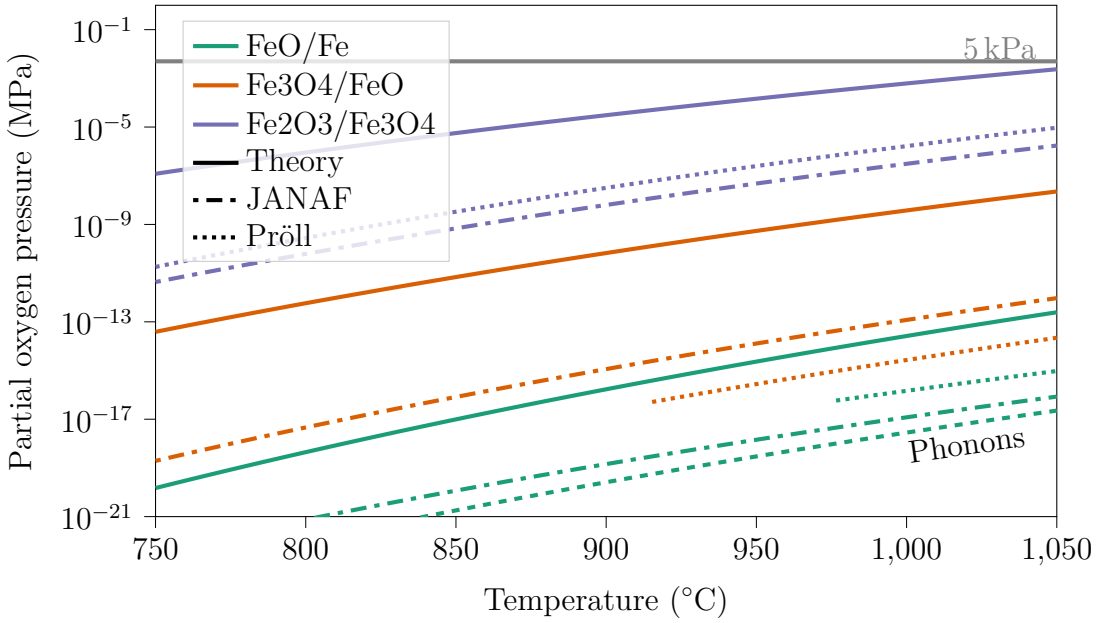

Figure 4.5: *Comparing different methods to acquire the transition energies. Here the special case for iron oxides is depicted in the associated modified Ellingham diagram. Each colour corresponds to a specific transition, while the different lines correspond to different methods. Fully drawn is the methodology developed in this thesis, dashed is with phonon corrections (only for* FeO/Fe*), dash-dotted from the Shomate equation and JANAF [63] and dotted from Pröll [65].*

In fig. 4.5 the iron oxide transitions are depicted in the associated modified Ellingham diagram. It is apparent that the order of the lines is consistent between different methods. Furthermore, the relative distance between the lines also seems to be somewhat consistent. However, the absolute placement of the lines seems to differ between the different methods. Especially the main method of this thesis denoted "Theory" in the legend of fig. 4.5 seems to be shifted upwards to higher partial pressure compared to the other methods. This can be interpreted that the magnitude of the transition energy is underestimated.

As the mean error is almost of the same order of magnitude as the RMSE (as can be in table 4.4) there is apparently some bias that appears from neglecting most of the differences in temperature dependence. This might actually be something positive, as this might indicate that the accuracy of the method could be improved by taking this bias into account as compared to a large random uncertainty which would be harder to adjust to.

Table 4.3: *The top ten highest ranked metal oxides for CLOU when filtered mono-, bi- and trimetalic compounds are considered.*

Place	Transition	Probability of crossing	Price $/kg	Oxygen transfer capacity	Score
1st	$4Fe_3O_4 + O_2 \leftrightharpoons 6Fe_2O_3$	0.478	0.0800	0.0148	443
2nd	$6FeO + O_2 \leftrightharpoons 2Fe_3O_4$	0.0904	0.0800	0.0318	180
3rd	$\frac{4}{3}Fe_2SiO_4 + \frac{4}{3}FeSiO_3 + O_2 \leftrightharpoons 2Fe_2O_3 + \frac{8}{3}SiO_2$	0.442	0.812	0.0178	48.4
4th	$\frac{1}{7}Zn_3Cu + \frac{1}{14}Zn_8Cu_5 + O_2 \leftrightharpoons \frac{1}{2}Zn_2CuO_4$	0.547	3.85	0.0631	44.8
5th	$4Fe_2O_3 + 4FeSiO_3 + O_2 \leftrightharpoons 6Fe_2O_3 + 4SiO_2$	0.531	0.538	0.007 62	37.6
6th	$\frac{1}{2}MgO + \frac{1}{7}Zn_3Cu + \frac{1}{14}Zn_8Cu_5 + O_2 \leftrightharpoons \frac{1}{2}MgO + \frac{1}{2}Zn_2CuO_4$	0.536	3.46	0.0420	32.6
7th	$4Fe_3O_4 + 3NaFeO_2 + O_2 \leftrightharpoons 6Fe_2O_3 + 3NaFeO_2$	0.455	0.573	0.008 03	31.9
8th	$\frac{12}{5}Fe_2SiO_4 + \frac{6}{5}FeSiO_3 + O_2 \leftrightharpoons 2Fe_3O_4 + \frac{18}{5}SiO_2$	0.377	0.766	0.0129	31.8
9th	$\frac{3}{28}Zn_{13}Fe + \frac{11}{28}ZnFe_2O_4 + O_2 \leftrightharpoons \frac{25}{28}Zn_2FeO_4$	0.311	1.91	0.0373	30.4
10th	$\frac{8}{23}Cu_2O + \frac{8}{23}Zn_3Cu + O_2 \leftrightharpoons \frac{6}{23}Cu_2O + \frac{12}{23}Zn_2CuO_4$	0.519	4.37	0.0498	29.6

Table 4.4: *Comparing generated transition energies (Theory) with transition energies from Pröll [65], JANAF [80] and in one case phonon corrected energies. The units for the energies are* eV/O_2 molecule *and therefore the same as equilibrium chemical potential of oxygen. At the bottom the differences are sumarised with the mean and the root mean square error (RMSE). Note that the theoretical values are constant as these are not mixes of compounds and therefore the mixing entropy is zero.*

Group	Specification	600 °C	750 °C	900 °C	1050 °C	1200 °C
Cu_2O/Cu	Theory	−4.11	−4.11	−4.11	−4.11	−4.11
	Pröll	−4.06	−4.21	−4.37	−4.53	−4.67
	JANAF	−4.14	−4.29	−4.45	−4.63	–
Co_3O_4/CoO	Theory	−3.75	−3.75	−3.75	−3.75	−3.75
	Pröll	−3.06	−2.91	−2.76	−2.63	–
	JANAF	−3.16	−3.01	−2.88	−2.77	−2.69
Mn_2O_3/Mn_3O_4	Theory	−2.46	−2.46	−2.46	−2.46	−2.46
	Pröll	−2.52	−2.65	−2.80	−2.95	−3.10
CuO/Cu_2O	Theory	−2.34	−2.34	−2.34	−2.34	−2.34
	Pröll	−2.91	−2.98	−3.07	−3.17	−3.26
	JANAF	−3.00	−3.07	−3.16	−3.26	−3.37
CuO/Cu	Theory	−3.22	−3.22	−3.22	−3.22	−3.22
	Pröll	−3.48	−3.59	−3.72	−3.85	−3.97
	JANAF	−3.57	−3.68	−3.81	−3.94	–
Fe_2O_3/Fe_3O_4	Theory	−3.46	−3.46	−3.46	−3.46	−3.46
	Pröll	−4.32	−4.24	−4.15	−4.09	−4.02
	JANAF	−4.43	−4.36	−4.32	−4.28	−4.26
Mn_3O_4/MnO	Theory	−4.58	−4.58	−4.58	−4.58	−4.58
	Pröll	−4.41	−4.41	−4.41	−4.44	−4.47
NiO/Ni	Theory	−4.97	−4.97	−4.97	−4.97	−4.97
	Pröll	–	−5.30	−5.41	−5.53	−5.66
CoO/Co	Theory	−5.02	−5.02	−5.02	−5.02	−5.02
	Pröll	–	–	−5.79	−5.96	−6.13
	JANAF	−5.54	−5.70	−5.87	−6.04	−6.22
Fe_3O_4/FeO	Theory	−4.78	−4.78	−4.78	−4.78	−4.78
	Pröll	–	–	–	−6.36	−6.44
	JANAF	−5.83	−5.85	−5.89	−5.93	−5.97
FeO/Fe	Theory	−6.08	−6.08	−6.08	−6.08	−6.08
	Phonons	−6.65	−6.80	−6.97	−7.14	−7.32
	Pröll	–	–	–	−6.71	−6.90
	JANAF	−6.42	−6.60	−6.79	−6.99	−7.19
Difference JANAF	Mean	0.42	0.48	0.55	0.64	0.71
	RMSE	0.65	0.71	0.80	0.90	1.07
Difference Phonons	Mean	0.57	0.72	0.89	1.06	1.24
	RMSE	0.57	0.72	0.89	1.06	1.24
Difference Pröll	Mean	0.12	0.18	0.29	0.50	0.76
	RMSE	0.48	0.50	0.60	0.81	0.87

Chapter 5

Reflection, further research and contributions

When faced with a difficult task it might be useful to simplify it to something that is workable. However, as a scientist it is important to never forget what assumptions lay the foundation for the conclusions. This is what we will explore in this part. As well as what has been done, what use it can be and how progress can continue.

5.1 Reflection

One of the very first assumption that was made was that thermodynamics and phase transitions determine what materials can be OCs. However, while seemingly reasonable this is not necessarily the whole truth. A material can release oxygen in other ways than undergoing a phase transition. Oxygen vacancies can form near the surface of the material and these vacancies can diffuse to the core bringing more oxygen atoms to the surface to be released to the air. This means that materials that are deemed impossible OCs for CLOU or any other CL process because of the lack of phase transition still retains some potential usefulness. Though the credence for this potential usefulness is reduced.

The other part of these two foundational assumptions is that thermodynamics is not the full part of the physical interaction that is relevant. Even if something is thermodynamically favoured it might still be kinetically hindered. The timescale of the transitions may be very long and the transitions therefore no longer of relevance. This is one of the major reasons that CLOU was chosen as a case study over other CL processes. As, if interactions with the fuel would have been necessary to reduce the OC, then this would increase the risk that kinetics would be an obstacle. However, even if there is some remaining risk that kinetics would render some OCs effectively inert, favourable thermodynamics is necessary for a phase transition to take place. Therefore, that a phase transition is thermodynamically favoured should significantly increase the credence that it is both thermodynamically favoured and kinetically enabled.

There have been several other assumptions and simplifications, both in the thermodynamic derivations and in the underlying ab-initio calculations. However, these have been investigated and compared with experimental sources. There was an in-

dication that the main cause of any uncertainty in the results were caused neglecting much of the differences in temperature dependence between different phases. Furthermore, it was discovered that the uncertainty seemed to be biased towards underestimating the energy released when an OC was oxidised. This is probably a good sign. Because, this means that there is some pattern in how the energies can be corrected. If there would be no pattern in the errors in the energy, then the only way to increase the accuracy would be to go to some higher order theory or experiments, which would defeat the whole point of this high-throughput screening, its speed.

Another thing to keep in mind is the roughness of the filters and in how the score is calculated. This could mean that some elements have been removed even though they might have been interesting or that some that remained is not feasible for some reason that was not caught in the filter. Luckily, the methodology can easily be adapted by tweaking the filters to something that would better correspond to what is wanted. Furthermore, one should keep in mind the size of the problem. This methodology has reduced roughly 10^8 possible phases (see eq. (2.1)) to around 6500 promising materials and ordered these after how promising they seem. This is no small task and accuracy have to be traded against computational speed.

5.2 Further research

There are a few possible directions for the path forward. The most obvious one is to do a more precise study of the most promising candidates both experimentally and with higher order theory. This would then give information into what the methodology is lacking and how as well as where improvements could be prioritised.

Before any detailed studies have been performed all that can be done is speculation. However, a few points seem especially important with regards to scope, neglectedness and tractability. By increasing the amount of transitions that is compared with experiments or whose phonon contributions are computed a better statistic could be acquired for the how the errors are distributed and the bias could easily be taken into account but more sophisticated models could also be used such as machine learning on the compositions to find a more fine tuned correction.

The durability of the OCs have only been investigated briefly. More effort could be put into finding a computationally cheap estimation of the durability. This could be from physical considerations[1] or by training a model on what experimental data can be found[2].

More oxides could be studied either by including more than trimetallic systems or by going beyond the ab-initio database to results from machine learning arbitrary compositions [85–87]. The main problem for this path is the increased computational cost when the considered phases increases.

[1] As the crystal structures are available in the database this could perhaps be based on metrics in similiarities of the phases [81–83].

[2] Could be similar to [84] but concentrated on durability.

5.3 Contributions

This thesis has developed and investigated a novel methodology for high-throughput screening from limited information. The computational cost is small, the screening is fast and it can be based on little more than the formation energies of compounds at a single reference temperature.

On the way the derivation of a simple and computationally cheap expression for a criterium of what enables CLOU has been performed. Furthermore, the accuracy of the expression has been investigated qualitatively, both compared to higher order theory and experimentally based expressions.

Reasonable filters have been applied based on the practical aspects of the process. Finally, a single quantifiable indicator has been proposed for how different promising OCs can be used compared against each other. This indicator have been used to rank all mono- and bimetallic materials in the OQMD as well as a filtered subset of mono-, bi and trimetallic materials in the database.

This screening methodology will hopefully speed up the search for new and better metal oxides for CL processes. Bringing a negative emission technology from a status as promising to actually economically viable.

Bibliography

[1] United Nations. *Paris Agreement*. 2015. URL: https://treaties.un.org/pages/ViewDetails.aspx?src=TREATY&mtdsg_no=XXVII-7-d&chapter=27&clang=_en (visited on 2020-04-21).

[2] Vera Heck et al. "Biomass-based negative emissions difficult to reconcile with planetary boundaries". In: *Nature Climate Change* 8.2 (2018-01), pp. 151–155.

[3] Johan Rockström et al. "A roadmap for rapid decarbonization". In: *Science* 355.6331 (2017-03), pp. 1269–1271.

[4] Sabine Fuss et al. "Betting on negative emissions". In: *Nature Climate Change* 4.10 (2014-09), pp. 850–853.

[5] T. Gasser et al. "Negative emissions physically needed to keep global warming below 2 °C". In: *Nature Communications* 6.1 (2015-08).

[6] Alexander Popp et al. "Land-use futures in the shared socio-economic pathways". In: *Global Environmental Change* 42 (2017-01), pp. 331–345.

[7] Carl-Friedrich Schleussner et al. "Science and policy characteristics of the Paris Agreement temperature goal". In: *Nature Climate Change* 6.9 (2016-07), pp. 827–835.

[8] Joeri Rogelj et al. "Energy system transformations for limiting end-of-century warming to below 1.5 °C". In: *Nature Climate Change* 5.6 (2015-05), pp. 519–527.

[9] K. Anderson and G. Peters. "The trouble with negative emissions". In: *Science* 354.6309 (2016-10), pp. 182–183.

[10] Dennis Y.C. Leung, Giorgio Caramanna, and M. Mercedes Maroto-Valer. "An overview of current status of carbon dioxide capture and storage technologies". In: *Renewable and Sustainable Energy Reviews* 39 (2014-11), pp. 426–443.

[11] M. Ishida, D. Zheng, and T. Akehata. "Evaluation of a chemical-looping-combustion power-generation system by graphic exergy analysis". In: *Energy* 12.2 (1987-02), pp. 147–154.

[12] Masaru Ishida and Hongguang Jin. "A novel combustor based on chemical-looping reactions and its reaction kinetics." In: *Journal of Chemical Engineering of Japan* 27.3 (1994), pp. 296–301.

[13] Xiao Zhao et al. "Biomass-based chemical looping technologies: the good, the bad and the future". In: *Energy & Environmental Science* 10.9 (2017), pp. 1885–1910.

[14] Liang Zeng et al. “Metal oxide redox chemistry for chemical looping processes”. In: *Nature Reviews Chemistry* 2.11 (2018-11), pp. 349–364.

[15] Lukas C. Buelens et al. “110th Anniversary: Carbon Dioxide and Chemical Looping: Current Research Trends”. In: *Industrial & Engineering Chemistry Research* 58.36 (2019-07), pp. 16235–16257.

[16] Xing Zhu et al. “Chemical looping beyond combustion – a perspective”. In: *Energy & Environmental Science* 13.3 (2020-03-18). Publisher: The Royal Society of Chemistry, pp. 772–804.

[17] Anders Lyngfelt and Hilmer Thunman. “Construction and 100 h of Operational Experience of A 10-kW Chemical-Looping Combustor”. In: *Carbon Dioxide Capture for Storage in Deep Geologic Formations*. Elsevier, 2005, pp. 625–645.

[18] Tobias Mattisson, Anders Lyngfelt, and Henrik Leion. “Chemical-looping with oxygen uncoupling for combustion of solid fuels”. In: *International Journal of Greenhouse Gas Control* 3.1 (2009-01), pp. 11–19.

[19] Tobias Mattisson et al. “Chemical-looping technologies using circulating fluidized bed systems: Status of development”. In: *Fuel Processing Technology* 172 (2018-04), pp. 1–12.

[20] Mehdi Arjmand et al. “Screening of Combined Mn-Fe-Si Oxygen Carriers for Chemical Looping with Oxygen Uncoupling (CLOU)”. In: *Energy & Fuels* 29.3 (2015-03), pp. 1868–1880.

[21] Axel D. Becke. “Perspective: Fifty years of density-functional theory in chemical physics”. In: *The Journal of Chemical Physics* 140.18 (2014-05), 18A301.

[22] Tanja van Mourik, Michael Bühl, and Marie-Pierre Gaigeot. “Density functional theory across chemistry, physics and biology”. In: *Philosophical Transactions of the Royal Society A: Mathematical, Physical and Engineering Sciences* 372.2011 (2014-03), p. 20120488.

[23] Claudia Draxl and Matthias Scheffler. “The NOMAD laboratory: from data sharing to artificial intelligence”. In: *Journal of Physics: Materials* 2.3 (2019-05), p. 036001.

[24] Stefano Curtarolo et al. “AFLOW: An automatic framework for high-throughput materials discovery”. In: *Computational Materials Science* 58 (2012-06), pp. 218–226.

[25] Stefano Curtarolo et al. “AFLOWLIB.ORG: A distributed materials properties repository from high-throughput ab initio calculations”. In: *Computational Materials Science* 58 (2012-06), pp. 227–235.

[26] James E. Saal et al. “Materials Design and Discovery with High-Throughput Density Functional Theory: The Open Quantum Materials Database (OQMD)”. In: *JOM* 65.11 (2013-09), pp. 1501–1509.

[27] Scott Kirklin et al. “The Open Quantum Materials Database (OQMD): assessing the accuracy of DFT formation energies”. In: *npj Computational Materials* 1.1 (2015-12).

[28] Anubhav Jain et al. “Commentary: The Materials Project: A materials genome approach to accelerating materials innovation”. In: *APL Materials* 1.1 (2013-07), p. 011002.

[29] Liang-Shih Fan, Liang Zeng, and Siwei Luo. “Chemical-looping technology platform”. In: *AIChE Journal* 61.1 (2015), pp. 2–22.

[30] Henrik Leion, Volkmar Frick, and Fredrik Hildor. “Experimental Method and Setup for Laboratory Fluidized Bed Reactor Testing”. In: *Energies* 11.10 (2018-09), p. 2505.

[31] A. Lyngfelt. “Oxygen carriers for chemical-looping combustion”. In: *Calcium and Chemical Looping Technology for Power Generation and Carbon Dioxide (CO2) Capture*. Elsevier, 2015, pp. 221–254.

[32] Antonio Saggion, Rossella Faraldo, and Matteo Pierno. “The Fundamental Relation and the Thermodynamic Potentials”. In: *UNITEXT for Physics*. Springer International Publishing, 2019, pp. 55–79.

[33] Carl R. Branan. “Properties”. In: *Rules of Thumb for Chemical Engineers*. Elsevier, 2005, pp. 390–425.

[34] Terrence L. Hill. *An Introduction to Statistical Thermodynamics*. Mineola, New York: Dover Publications, 1986.

[35] R.P. Feynman, R.B. Leighton, and M. Sands. *The Feynman Lectures on Physics, Vol. I: The New Millennium Edition: Mainly Mechanics, Radiation, and Heat*. Vol. 1. Basic Books, 2015.

[36] Karsten Reuter and Matthias Scheffler. “Composition, structure, and stability of RuO_2(110) as a function of oxygen pressure”. In: *Physical Review B* 65 (2001-12-19).

[37] E. Schrödinger. “Quantisierung als Eigenwertproblem”. In: *Annalen der Physik* 385.13 (1926), pp. 437–490.

[38] P. Hohenberg and W. Kohn. “Inhomogeneous Electron Gas”. In: *Physical Review* 136.3B (1964-11), B864–B871.

[39] W. Kohn and L. J. Sham. “Self-Consistent Equations Including Exchange and Correlation Effects”. In: *Physical Review* 140.4A (1965-11), A1133–A1138.

[40] Adam A Arvidsson. “Partial methane oxidation: insights from first principles and micro-kinetics calculations”. Text in English. Summary given in Swedish. OCLC: 1120216594. PhD thesis. Chalmers University of Technology, 2019.

[41] Anders Hellman. “Electron Transfer and Molecular Dynamics at Metal Surfaces”. PhD thesis. Chalmers University of Technology, 2003.

[42] John P. Perdew, Kieron Burke, and Matthias Ernzerhof. “Generalized Gradient Approximation Made Simple”. In: *Physical Review Letters* 77.18 (1996-10), pp. 3865–3868.

[43] J. J. Mortensen et al. “Bayesian Error Estimation in Density-Functional Theory”. In: *Physical Review Letters* 95.21 (2005-11).

[44] Sarah A. Tolba et al. “The DFT+U: Approaches, Accuracy, and Applications”. In: *Density Functional Calculations - Recent Progresses of Theory and Application*. InTech, 2018-05.

[45] A. I. Liechtenstein, V. I. Anisimov, and J. Zaanen. “Density-functional theory and strong interactions: Orbital ordering in Mott-Hubbard insulators”. In: *Physical Review B* 52.8 (1995-08), R5467–R5470.

[46] S. L. Dudarev et al. “Electron-energy-loss spectra and the structural stability of nickel oxide: An LSDA+U study”. In: *Physical Review B* 57.3 (1998-01), pp. 1505–1509.

[47] Vladan Stevanović et al. “Correcting density functional theory for accurate predictions of compound enthalpies of formation: Fitted elemental-phase reference energies”. In: *Physical Review B* 85.11 (2012-03).

[48] Dario Alfè. “PHON: A program to calculate phonons using the small displacement method”. In: *Computer Physics Communications* 180.12 (2009-12), pp. 2622–2633.

[49] Donald Allan McQuarrie. *Statistical Mechanics*. Harper’s Chemistry Series. New York: HarperCollins Publishing, Inc., 1976.

[50] Peter J. Linstrom and William G. Mallard. “The NIST Chemistry WebBook: A Chemical Data Resource on the Internet†”. In: *Journal of Chemical & Engineering Data* 46.5 (2001-09), pp. 1059–1063.

[51] Guido Van Rossum and Fred L. Drake. *Python 3 Reference Manual*. Scotts Valley, CA: CreateSpace, 2009.

[52] Stéfan van der Walt, S Chris Colbert, and Gaël Varoquaux. “The NumPy Array: A Structure for Efficient Numerical Computation”. In: *Computing in Science & Engineering* 13.2 (2011-03), pp. 22–30.

[53] Pauli Virtanen et al. “SciPy 1.0: Fundamental Algorithms for Scientific Computing in Python”. In: *Nature Methods* 17 (2020), pp. 261–272.

[54] John D. Hunter. “Matplotlib: A 2D Graphics Environment”. In: *Computing in Science & Engineering* 9.3 (2007), pp. 90–95.

[55] Michael Waskom et al. *mwaskom/seaborn: v0.8.1 (September 2017)*. Version v0.8.1. 2017-09. URL: `https://doi.org/10.5281/zenodo.883859`.

[56] Nico Schlömer et al. *nschloe/tikzplotlib 0.9.1*. 2020. URL: `https://zenodo.org/record/3633995`.

[57] Wes McKinney. “Data Structures for Statistical Computing in Python”. In: *Proceedings of the 9th Python in Science Conference*. Ed. by Stéfan van der Walt and Jarrod Millman. 2010, pp. 56–61.

[58] D.R. Gaskell. “Metal Production: Ellingham Diagrams”. In: *Encyclopedia of Materials: Science and Technology*. Elsevier, 2001, pp. 5481–5486.

[59] Charles Kittel. *Introduction to Solid State Physics*. Eight.

[60] D. D. Lee, J. H. Choy, and J. K. Lee. “Computer generation of binary and ternary phase diagrams via a convex hull method”. In: *Journal of Phase Equilibria* 13.4 (1992-08), pp. 365–372.

[61] D. Hildebrandt and D. Glasser. “Predicting phase and chemical equilibrium using the convex hull of the Gibbs free energy”. In: *The Chemical Engineering Journal and the Biochemical Engineering Journal* 54.3 (1994-07), pp. 187–197.

[62] Antoine A. Emery and Chris Wolverton. “High-throughput DFT calculations of formation energy, stability and oxygen vacancy formation energy of ABO3 perovskites”. In: *Scientific Data* 4.1 (2017-10).

[63] Malcolm W. Chase Jr. *NIST-JANAF Thermochemical Tables*. Fourth. Gaithersburg, Maryland: National Institute of Standards and Technology.

[64] Harold J. T. Ellingham. “Reducibility of oxides and sulphides in metallurgical processes”. In: *Journal of the Society of Chemical Industry* 63.5 (1944), pp. 125–160.

[65] T. Pröll. “10 - Fundamentals of chemical looping combustion and introduction to CLC reactor design”. In: *Calcium and Chemical Looping Technology for Power Generation and Carbon Dioxide (CO2) Capture*. Ed. by Paul Fennell and Ben Anthony. Woodhead Publishing Series in Energy. Woodhead Publishing, 2015-01-01, pp. 197–219.

[66] Andy Brunning. *Periodic Table of Element Hazard Symbols*. 2019. URL: `https://www.compoundchem.com/2019advent/day15/` (visited on 2020-05-14).

[67] European Chemical Society. *Element Scarcity – EuChemS Periodic Table*. 2019. URL: `https://www.euchems.eu/euchems-periodic-table/` (visited on 2020-05-14).

[68] Wikipedia. *Chemical element*. 2020. URL: `http://en.wikipedia.org/w/index.php?title=Chemical%5C%20element&oldid=955010209` (visited on 2020-05-14).

[69] Leonland. *Chemical elements by market price*. 2018. URL: `http://www.leonland.de/elements_by_price/en/list` (visited on 2020-05-14).

[70] Angstrom Sciences. *Melting Points of Elements Reference*. URL: `https://www.angstromsciences.com/melting-points-of-elements-reference` (visited on 2020-05-21).

[71] Anders Lyngfelt and Bo Leckner. “A 1000 MWth boiler for chemical-looping combustion of solid fuels – Discussion of design and costs”. In: *Applied Energy* 157 (2015-11), pp. 475–487.

[72] Ask Hjorth Larsen et al. “The atomic simulation environment—a Python library for working with atoms”. In: *Journal of Physics: Condensed Matter* 29.27 (2017), p. 273002.

[73] G. Kresse and J. Hafner. “Ab initiomolecular dynamics for liquid metals”. In: *Physical Review B* 47.1 (1993-01), pp. 558–561.

[74] G. Kresse and J. Hafner. “Ab initiomolecular-dynamics simulation of the liquid-metal–amorphous-semiconductor transition in germanium”. In: *Physical Review B* 49.20 (1994-05), pp. 14251–14269.

[75] G. Kresse and J. Furthmüller. “Efficiency of ab-initio total energy calculations for metals and semiconductors using a plane-wave basis set”. In: *Computational Materials Science* 6.1 (1996-07), pp. 15–50.

[76] G. Kresse and J. Furthmüller. “Efficient iterative schemes forab initiototal-energy calculations using a plane-wave basis set”. In: *Physical Review B* 54.16 (1996-10), pp. 11169–11186.

[77] P. E. Blöchl. “Projector augmented-wave method”. In: *Physical Review B* 50.24 (1994-12), pp. 17953–17979.

[78] G. Kresse and D. Joubert. “From ultrasoft pseudopotentials to the projector augmented-wave method”. In: *Physical Review B* 59.3 (1999-01), pp. 1758–1775.

[79] J. P. Perdew, K. Burke, and M. Ernzerhof. “Errata: Generalized Gradient Approximation Made Simple”. In: *Phys. Rev. Lett.* 78 (1996).

[80] Tom Allison. *JANAF Thermochemical Tables, NIST Standard Reference Database 13*. eng. 1996. URL: `http://kinetics.nist.gov/janaf/`.

[81] Li Zhu et al. “A fingerprint based metric for measuring similarities of crystalline structures”. In: *The Journal of Chemical Physics* 144.3 (2016-01), p. 034203.

[82] Gemma de la Flor et al. “Comparison of structures applying the tools available at the Bilbao Crystallographic Server”. In: *Journal of Applied Crystallography* 49.2 (2016-03), pp. 653–664.

[83] Alireza Khorshidi and Andrew A. Peterson. “Amp: A modular approach to machine learning in atomistic simulations”. In: *Computer Physics Communications* 207 (2016-10), pp. 310–324.

[84] Yongliang Yan et al. “Applying machine learning algorithms in estimating the performance of heterogeneous, multi-component materials as oxygen carriers for chemical-looping processes”. In: *Chemical Engineering Journal* 387 (2020-05), p. 124072.

[85] B. Meredig et al. “Combinatorial screening for new materials in unconstrained composition space with machine learning”. In: *Physical Review B* 89.9 (2014-03).

[86] Ankit Agrawal et al. “A Formation Energy Predictor for Crystalline Materials Using Ensemble Data Mining”. In: *2016 IEEE 16th International Conference on Data Mining Workshops (ICDMW)*. IEEE, 2016-12.

[87] Dipendra Jha et al. “ElemNet: Deep Learning the Chemistry of Materials From Only Elemental Composition”. In: *Scientific Reports* 8.1 (2018-12).

Appendix A

Extended ranking lists

This appendix includes extended ranking lists.

A.1 Ranking for filtered monometallic CLOU transitions

The complete ranking of filtered monometallic CLOU transitions.

Place	Transition	Probability of crossing	Price $/kg	Oxygen transfer capacity	Score
1st	$4Fe_3O_4 + O_2 \leftrightharpoons 6Fe_2O_3$	0.478	0.0800	0.0148	443
2nd	$6FeO + O_2 \leftrightharpoons 2Fe_3O_4$	0.0904	0.0800	0.0318	180
3rd	$2Fe + O_2 \leftrightharpoons 2FeO$	0.003 59	0.0800	0.111	25
4th	$2Cu_2O + O_2 \leftrightharpoons 4CuO$	0.450	5.90	0.0503	19.2
5th	$4Mn_3O_4 + O_2 \leftrightharpoons 6Mn_2O_3$	0.485	2.06	0.0150	17.7
6th	$4Cu + O_2 \leftrightharpoons 2Cu_2O$	0.262	5.90	0.0670	14.9
7th	$6MnO + O_2 \leftrightharpoons 2Mn_3O_4$	0.130	2.06	0.0322	10.1
8th	$2SrO + O_2 \leftrightharpoons 2SrO_2$	0.100	5.40	0.0515	4.78
9th	$2Mn_2O_3 + O_2 \leftrightharpoons 4MnO_2$	0.0511	2.06	0.0376	4.66

Continued on next page

Place	Transition	Probability of crossing	Price $/kg	Oxygen transfer capacity	Score
10th	$2Sb_2O_3 + O_2 \leftrightharpoons 4SbO_2$	0.288	7.05	0.0194	3.95
11th	$4SbO_2 + O_2 \leftrightharpoons 2Sb_2O_5$	0.291	7.05	0.0166	3.43
12th	$2MgO + O_2 \leftrightharpoons 2MgO_2$	0.0104	2.26	0.132	3.05
13th	$\frac{10}{3}V_2O_3 + O_2 \leftrightharpoons \frac{4}{3}V_5O_9$	0.365	22.6	0.0256	2.07
14th	$2MoO_2 + O_2 \leftrightharpoons 2MoO_3$	0.180	16	0.0357	2.01
15th	$4VO_2 + O_2 \leftrightharpoons 2V_2O_5$	0.217	22.6	0.0341	1.64
16th	$\frac{4}{3}Sb + O_2 \leftrightharpoons \frac{2}{3}Sb_2O_3$	0.0321	7.05	0.0697	1.59
17th	$2V_5O_9 + O_2 \leftrightharpoons 10VO_2$	0.427	22.6	0.0159	1.50
18th	$2CaO + O_2 \leftrightharpoons 2CaO_2$	0.0127	5.93	0.0951	1.01
19th	$2Cr_2O_3 + O_2 \leftrightharpoons 4CrO_2$	0.0237	7.64	0.0392	0.609
20th	$2Nd_2O_3 + O_2 \leftrightharpoons 4NdO_2$	0.118	60	0.0166	0.164
21st	$2BaO + O_2 \leftrightharpoons 2BaO_2$	0.323	550	0.0348	0.102
22nd	$4Ag + O_2 \leftrightharpoons 2Ag_2O$	0.149	462	0.0431	0.0696
23rd	$Mo + O_2 \leftrightharpoons MoO_2$	0.001 04	16	0.0953	0.0310
24th	$2Ag_2O + O_2 \leftrightharpoons 4AgO$	0.0390	462	0.0323	0.0136
25th	$6AgO + O_2 \leftrightharpoons 2Ag_3O_4$	0.0109	462	0.0185	0.002 18
26th	$2Ti_3O_5 + O_2 \leftrightharpoons 6TiO_2$	1.26×10^{-5}	3.77	0.0278	0.000 465

Continued on next page

Place	Transition	Probability of crossing	Price $/kg	Oxygen transfer capacity	Score
27th	$4NbO_2 + O_2 \leftrightharpoons 2Nb_2O_5$	0.000 113	42	0.0210	0.000 282
28th	$2Mn + O_2 \leftrightharpoons 2MnO$	9.03×10^{-7}	2.06	0.113	0.000 247
29th	$6Ti_2O_3 + O_2 \leftrightharpoons 4Ti_3O_5$	3.08×10^{-6}	3.77	0.0157	6.40×10^{-5}
30th	$2NbO + O_2 \leftrightharpoons 2NbO_2$	7.90×10^{-6}	42	0.0490	4.61×10^{-5}
31st	$\frac{4}{3}Cr + O_2 \leftrightharpoons \frac{2}{3}Cr_2O_3$	4.87×10^{-7}	7.64	0.141	4.50×10^{-5}
32nd	$4VO + O_2 \leftrightharpoons 2V_2O_3$	6.96×10^{-7}	22.6	0.0478	7.36×10^{-6}
33rd	$Si + O_2 \leftrightharpoons SiO_2$	2.52×10^{-9}	1.91	0.242	1.59×10^{-6}
34th	$2Nb + O_2 \leftrightharpoons 2NbO$	7.83×10^{-8}	42	0.0735	6.85×10^{-7}
35th	$2V + O_2 \leftrightharpoons 2VO$	6.87×10^{-9}	22.6	0.120	1.82×10^{-7}
36th	$4TiO + O_2 \leftrightharpoons 2Ti_2O_3$	1.79×10^{-9}	3.77	0.0501	1.19×10^{-7}
37th	$2Ti_2O + O_2 \leftrightharpoons 4TiO$	1.47×10^{-11}	3.77	0.0626	1.22×10^{-9}
38th	$\frac{4}{3}Al + O_2 \leftrightharpoons \frac{2}{3}Al_2O_3$	2.97×10^{-14}	1.91	0.223	1.74×10^{-11}
39th	$\frac{2}{5}Zr_3O + O_2 \leftrightharpoons \frac{6}{5}ZrO_2$	1.08×10^{-13}	23.1	0.0829	1.93×10^{-12}
40th	$4Ti_3O + O_2 \leftrightharpoons 6Ti_2O$	1.70×10^{-14}	3.77	0.0278	6.26×10^{-13}
41st	$2Ba + O_2 \leftrightharpoons 2BaO$	8.59×10^{-14}	550	0.0522	4.07×10^{-14}
42nd	$2Mg + O_2 \leftrightharpoons 2MgO$	2.03×10^{-17}	2.26	0.198	8.91×10^{-15}
43rd	$2Sr + O_2 \leftrightharpoons 2SrO$	2.08×10^{-17}	5.40	0.0772	1.48×10^{-15}

Continued on next page

Place	Transition	Probability of crossing	Price $/kg	Oxygen transfer capacity	Score
44th	$\frac{4}{3}Ce + O_2 \leftrightharpoons \frac{2}{3}Ce_2O_3$	3.12×10^{-17}	7	0.0615	1.37×10^{-15}
45th	$2Ti_6O + O_2 \leftrightharpoons 4Ti_3O$	3.08×10^{-17}	3.77	0.0313	1.28×10^{-15}
46th	$6Zr + O_2 \leftrightharpoons 2Zr_3O$	1.38×10^{-17}	23.1	0.0373	1.11×10^{-16}
47th	$\frac{4}{3}Nd + O_2 \leftrightharpoons \frac{2}{3}Nd_2O_3$	1.75×10^{-18}	60	0.0599	8.72×10^{-18}
48th	$\frac{4}{3}Tb + O_2 \leftrightharpoons \frac{2}{3}Tb_2O_3$	1×10^{-17}	550	0.0549	5×10^{-18}
49th	$\frac{4}{3}La + O_2 \leftrightharpoons \frac{2}{3}La_2O_3$	1.12×10^{-19}	7	0.0620	4.94×10^{-18}
50th	$\frac{4}{3}Sm + O_2 \leftrightharpoons \frac{2}{3}Sm_2O_3$	1.58×10^{-19}	14.4	0.0577	3.18×10^{-18}
51st	$2Ca + O_2 \leftrightharpoons 2CaO$	2.49×10^{-21}	5.93	0.143	2.99×10^{-19}
52nd	$\frac{4}{3}Y + O_2 \leftrightharpoons \frac{2}{3}Y_2O_3$	5.81×10^{-21}	35	0.0915	7.60×10^{-20}
53rd	$\frac{4}{3}Gd + O_2 \leftrightharpoons \frac{2}{3}Gd_2O_3$	9.47×10^{-21}	55	0.0554	4.77×10^{-20}
54th	$12Ti + O_2 \leftrightharpoons 2Ti_6O$	1.69×10^{-22}	3.77	0.0358	8.04×10^{-21}
55th	$\frac{4}{3}Dy + O_2 \leftrightharpoons \frac{2}{3}Dy_2O_3$	1.55×10^{-21}	350	0.0538	1.19×10^{-21}
56th	$\frac{4}{3}Er + O_2 \leftrightharpoons \frac{2}{3}Er_2O_3$	3.46×10^{-22}	95	0.0524	9.54×10^{-22}

Continued on next page

Place	Transition	Probability of crossing	Price $/kg	Oxygen transfer capacity	Score
57^{th}	$2\text{Eu} + \text{O}_2 \leftrightharpoons 2\text{EuO}$	8.76×10^{-25}	258	0.0476	8.08×10^{-25}

A.2 Ranking for unfiltered monometallic CLOU transitions

The complete ranking of unfiltered monometallic CLOU transitions.

Place	Transition	Probability of crossing	Price $/kg	Oxygen transfer capacity	Score
1st	$4Fe_3O_4 + O_2 \leftrightharpoons 6Fe_2O_3$	0.478	0.0800	0.0148	443
2nd	$6FeO + O_2 \leftrightharpoons 2Fe_3O_4$	0.0904	0.0800	0.0318	180
3rd	$2Na_2O + O_2 \leftrightharpoons 4NaO$	0.367	3.04	0.103	61.9
4th	$As_2O_3 + O_2 \leftrightharpoons As_2O_5$	0.427	1.74	0.0503	61.7
5th	$\frac{4}{3}As + O_2 \leftrightharpoons \frac{2}{3}As_2O_3$	0.0832	1.74	0.106	25.2
6th	$2Fe + O_2 \leftrightharpoons 2FeO$	0.003 59	0.0800	0.111	25
7th	$2Cu_2O + O_2 \leftrightharpoons 4CuO$	0.450	5.90	0.0503	19.2
8th	$4Mn_3O_4 + O_2 \leftrightharpoons 6Mn_2O_3$	0.485	2.06	0.0150	17.7
9th	$2K_2O + O_2 \leftrightharpoons 4KO$	0.543	13.0	0.0726	15.1
10th	$4Cu + O_2 \leftrightharpoons 2Cu_2O$	0.262	5.90	0.0670	14.9
11th	$2NaO + O_2 \leftrightharpoons 2NaO_2$	0.0627	3.04	0.137	14.1
12th	$6MnO + O_2 \leftrightharpoons 2Mn_3O_4$	0.130	2.06	0.0322	10.1
13th	$2Cd + O_2 \leftrightharpoons 2CdO$	0.0631	1.98	0.0623	9.93
14th	$6PbO + O_2 \leftrightharpoons 2Pb_3O_4$	0.381	2.29	0.0102	8.52
15th	$2NaO_2 + O_2 \leftrightharpoons 2NaO_3$	0.0463	3.04	0.103	7.81

Continued on next page

Place	Transition	Probability of crossing	Price $/kg	Oxygen transfer capacity	Score
16th	$2KO + O_2 \leftrightharpoons 2KO_2$	0.156	13.0	0.0968	5.80
17th	$2SrO + O_2 \leftrightharpoons 2SrO_2$	0.100	5.40	0.0515	4.78
18th	$2Mn_2O_3 + O_2 \leftrightharpoons 4MnO_2$	0.0511	2.06	0.0376	4.66
19th	$2Sb_2O_3 + O_2 \leftrightharpoons 4SbO_2$	0.288	7.05	0.0194	3.95
20th	$2Ni + O_2 \leftrightharpoons 2NiO$	0.0621	9.19	0.107	3.62
21st	$4SbO_2 + O_2 \leftrightharpoons 2Sb_2O_5$	0.291	7.05	0.0166	3.43
22nd	$2MgO + O_2 \leftrightharpoons 2MgO_2$	0.0104	2.26	0.132	3.05
23rd	$Pb_3O_4 + O_2 \leftrightharpoons 3PbO_2$	0.0815	2.29	0.0159	2.84
24th	$2Pb + O_2 \leftrightharpoons 2PbO$	0.0306	2.29	0.0358	2.40
25th	$Te + O_2 \leftrightharpoons TeO_2$	0.333	55.7	0.0743	2.22
26th	$\frac{10}{3}V_2O_3 + O_2 \leftrightharpoons \frac{4}{3}V_5O_9$	0.365	22.6	0.0256	2.07
27th	$2MoO_2 + O_2 \leftrightharpoons 2MoO_3$	0.180	16	0.0357	2.01
28th	$4VO_2 + O_2 \leftrightharpoons 2V_2O_5$	0.217	22.6	0.0341	1.64
29th	$\frac{4}{3}Sb + O_2 \leftrightharpoons \frac{2}{3}Sb_2O_3$	0.0321	7.05	0.0697	1.59
30th	$2V_5O_9 + O_2 \leftrightharpoons 10VO_2$	0.427	22.6	0.0159	1.50
31st	$\frac{4}{3}Bi + O_2 \leftrightharpoons \frac{2}{3}Bi_2O_3$	0.0692	10.3	0.0427	1.43
32nd	$2Hg + O_2 \leftrightharpoons 2HgO$	0.272	38.4	0.0369	1.31

Continued on next page

Place	Transition	Probability of crossing	Price $/kg	Oxygen transfer capacity	Score
33rd	$2CaO + O_2 \leftrightharpoons 2CaO_2$	0.0127	5.93	0.0951	1.01
34th	$6CoO + O_2 \leftrightharpoons 2Co_3O_4$	0.387	59.5	0.0305	0.991
35th	$2KO_2 + O_2 \leftrightharpoons 2KO_3$	0.0271	13.0	0.0726	0.755
36th	$2NiO + O_2 \leftrightharpoons 2NiO_2$	0.0185	9.19	0.0714	0.721
37th	$2Li_2O + O_2 \leftrightharpoons 4LiO$	0.0853	116	0.174	0.643
38th	$2Cr_2O_3 + O_2 \leftrightharpoons 4CrO_2$	0.0237	7.64	0.0392	0.609
39th	$2Co + O_2 \leftrightharpoons 2CoO$	0.0556	59.5	0.107	0.499
40th	$3UO_2 + O_2 \leftrightharpoons U_3O_8$	0.486	57.8	0.0115	0.481
41st	$4Bi_2O_3 + O_2 \leftrightharpoons 2Bi_4O_7$	0.126	10.3	0.006 46	0.394
42nd	$2LiO + O_2 \leftrightharpoons 2LiO_2$	0.0352	116	0.232	0.354
43rd	$4TeO_2 + O_2 \leftrightharpoons 2Te_2O_5$	0.128	55.7	0.0159	0.183
44th	$2Nd_2O_3 + O_2 \leftrightharpoons 4NdO_2$	0.118	60	0.0166	0.164
45th	$2SnO + O_2 \leftrightharpoons 2SnO_2$	0.0151	20	0.0396	0.149
46th	$2Zn + O_2 \leftrightharpoons 2ZnO$	0.000 660	2.83	0.0983	0.115
47th	$2BaO + O_2 \leftrightharpoons 2BaO_2$	0.323	550	0.0348	0.102
48th	$2LiO_2 + O_2 \leftrightharpoons 2LiO_3$	0.0108	116	0.174	0.0815
49th	$2U_3O_8 + O_2 \leftrightharpoons 6UO_3$	0.166	57.8	0.005 25	0.0753
50th	$4Ag + O_2 \leftrightharpoons 2Ag_2O$	0.149	462	0.0431	0.0696

Continued on next page

Place	Transition	Probability of crossing	Price $/kg	Oxygen transfer capacity	Score
51st	$2Te_2O_5 + O_2 \leftrightharpoons 4TeO_3$	0.0450	55.7	0.0139	0.0562
52nd	$Ru + O_2 \leftrightharpoons RuO_2$	0.367	3050	0.0911	0.0547
53rd	$2Sn + O_2 \leftrightharpoons 2SnO$	0.002 91	20	0.0594	0.0432
54th	$Mo + O_2 \leftrightharpoons MoO_2$	0.001 04	16	0.0953	0.0310
55th	$2Bi_4O_7 + O_2 \leftrightharpoons 8BiO_2$	0.007 39	10.3	0.005 93	0.0212
56th	$2Ag_2O + O_2 \leftrightharpoons 4AgO$	0.0390	462	0.0323	0.0136
57th	$W + O_2 \leftrightharpoons WO_2$	0.000 829	25.5	0.0534	0.008 67
58th	$Re + O_2 \leftrightharpoons ReO_2$	0.0443	1640	0.0527	0.007 15
59th	$\frac{2}{3}Tl_4O_3 + O_2 \leftrightharpoons \frac{4}{3}Tl_2O_3$	0.486	7400	0.0218	0.007 15
60th	$2Rb_2O + O_2 \leftrightharpoons 4RbO$	0.510	14 700	0.0394	0.006 83
61st	$4K + O_2 \leftrightharpoons 2K_2O$	0.000 158	13.0	0.0968	0.005 87
62nd	$2Pd + O_2 \leftrightharpoons 2PdO$	0.517	34 400	0.0653	0.004 91
63rd	$Ir + O_2 \leftrightharpoons IrO_2$	0.536	31 200	0.0512	0.004 40
64th	$Ge + O_2 \leftrightharpoons GeO_2$	0.0117	1830	0.120	0.003 86
65th	$2ReO_2 + O_2 \leftrightharpoons 2ReO_3$	0.0632	1640	0.0198	0.003 82
66th	$\frac{3}{2}Pt + O_2 \leftrightharpoons \frac{1}{2}Pt_3O_4$	0.458	26 500	0.0433	0.003 74
67th	$4Tl_2O + O_2 \leftrightharpoons 2Tl_4O_3$	0.534	7400	0.0104	0.003 74

Continued on next page

Place	Transition	Probability of crossing	Price $/kg	Oxygen transfer capacity	Score
68th	$2WO_2 + O_2 \leftrightharpoons 2WO_3$	0.000 903	25.5	0.0200	0.003 54
69th	$Rh + O_2 \leftrightharpoons RhO_2$	0.545	76 800	0.0897	0.003 18
70th	$4Tl + O_2 \leftrightharpoons 2Tl_2O$	0.193	7400	0.0242	0.003 15
71st	$\frac{4}{3}In + O_2 \leftrightharpoons \frac{2}{3}In_2O_3$	0.002 92	342	0.0734	0.003 14
72nd	$4ReO_3 + O_2 \leftrightharpoons 2Re_2O_7$	0.107	1640	0.008 79	0.002 88
73rd	$4RbO + O_2 \leftrightharpoons 2Rb_2O_3$	0.251	14 700	0.0315	0.002 69
74th	$RuO_2 + O_2 \leftrightharpoons RuO_4$	0.0253	3050	0.0547	0.002 26
75th	$6AgO + O_2 \leftrightharpoons 2Ag_3O_4$	0.0109	462	0.0185	0.002 18
76th	$2YbO + O_2 \leftrightharpoons 2YbO_2$	0.0179	1600	0.0282	0.001 58
77th	$2Rb_2O_3 + O_2 \leftrightharpoons 4RbO_2$	0.138	14 700	0.0263	0.001 23
78th	$2Cs_2O + O_2 \leftrightharpoons 4CsO$	0.552	73 400	0.0269	0.001 01
79th	$Pt_3O_4 + O_2 \leftrightharpoons 3PtO_2$	0.311	26 500	0.0168	0.000 988
80th	$2CsO + O_2 \leftrightharpoons 2CsO_2$	0.195	73 400	0.0358	0.000 475
81st	$2Ti_3O_5 + O_2 \leftrightharpoons 6TiO_2$	1.26×10^{-5}	3.77	0.0278	0.000 465
82nd	$2RbO_2 + O_2 \leftrightharpoons 2RbO_3$	0.0339	14 700	0.0394	0.000 454
83rd	$\frac{4}{3}Au + O_2 \leftrightharpoons \frac{2}{3}Au_2O_3$	0.0631	38 200	0.0451	0.000 373
84th	$4PdO + O_2 \leftrightharpoons 2Pd_2O_3$	0.0836	34 400	0.0261	0.000 318

Continued on next page

Place	Transition	Probability of crossing	Price $/kg	Oxygen transfer capacity	Score
85th	$\frac{4}{3}Ga + O_2 \leftrightharpoons \frac{2}{3}Ga_2O_3$	0.000 146	278	0.112	0.000 294
86th	$4NbO_2 + O_2 \leftrightharpoons 2Nb_2O_5$	0.000 113	42	0.0210	0.000 282
87th	$2Mn + O_2 \leftrightharpoons 2MnO$	9.03×10^{-7}	2.06	0.113	0.000 247
88th	$\frac{4}{5}Rb_9O_2 + O_2 \leftrightharpoons \frac{18}{5}Rb_2O$	0.007 15	14 700	0.0292	7.09×10^{-5}
89th	$6Ti_2O_3 + O_2 \leftrightharpoons 4Ti_3O_5$	3.08×10^{-6}	3.77	0.0157	6.40×10^{-5}
90th	$2CsO_2 + O_2 \leftrightharpoons 2CsO_3$	0.0304	73 400	0.0269	5.56×10^{-5}
91st	$2NbO + O_2 \leftrightharpoons 2NbO_2$	7.90×10^{-6}	42	0.0490	4.61×10^{-5}
92nd	$\frac{4}{3}Cr + O_2 \leftrightharpoons \frac{2}{3}Cr_2O_3$	4.87×10^{-7}	7.64	0.141	4.50×10^{-5}
93rd	$2Pd_2O_3 + O_2 \leftrightharpoons 4PdO_2$	0.0118	34 400	0.0218	3.75×10^{-5}
94th	$4Na + O_2 \leftrightharpoons 2Na_2O$	1.01×10^{-7}	3.04	0.137	2.28×10^{-5}
95th	$4VO + O_2 \leftrightharpoons 2V_2O_3$	6.96×10^{-7}	22.6	0.0478	7.36×10^{-6}
96th	$9Rb + O_2 \leftrightharpoons Rb_9O_2$	0.000 277	14 700	0.0287	2.70×10^{-6}
97th	$\frac{4}{5}Cs_7O + O_2 \leftrightharpoons \frac{14}{5}Cs_2O$	0.001 04	73 400	0.0256	1.80×10^{-6}
98th	$Si + O_2 \leftrightharpoons SiO_2$	2.52×10^{-9}	1.91	0.242	1.59×10^{-6}
99th	$2Nb + O_2 \leftrightharpoons 2NbO$	7.83×10^{-8}	42	0.0735	6.85×10^{-7}
100th	$2V + O_2 \leftrightharpoons 2VO$	6.87×10^{-9}	22.6	0.120	1.82×10^{-7}

Continued on next page

Place	Transition	Probability of crossing	Price $/kg	Oxygen transfer capacity	Score
101st	$4TiO + O_2 \leftrightharpoons 2Ti_2O_3$	1.79×10^{-9}	3.77	0.0501	1.19×10^{-7}
102nd	$\frac{1}{4}B_6O + O_2 \leftrightharpoons \frac{3}{4}B_2O_3$	1.55×10^{-7}	2390	0.318	1.03×10^{-7}
103rd	$14Cs + O_2 \leftrightharpoons 2Cs_7O$	8.14×10^{-5}	73 400	0.0134	7.44×10^{-8}
104th	$\frac{4}{5}Ta + O_2 \leftrightharpoons \frac{2}{5}Ta_2O_5$	3.53×10^{-8}	238	0.0580	4.30×10^{-8}
105th	$2Ti_2O + O_2 \leftrightharpoons 4TiO$	1.47×10^{-11}	3.77	0.0626	1.22×10^{-9}
106th	$\frac{4}{3}Al + O_2 \leftrightharpoons \frac{2}{3}Al_2O_3$	2.97×10^{-14}	1.91	0.223	1.74×10^{-11}
107th	$\frac{2}{5}Zr_3O + O_2 \leftrightharpoons \frac{6}{5}ZrO_2$	1.08×10^{-13}	23.1	0.0829	1.93×10^{-12}
108th	$4Ti_3O + O_2 \leftrightharpoons 6Ti_2O$	1.70×10^{-14}	3.77	0.0278	6.26×10^{-13}
109th	$2Ba + O_2 \leftrightharpoons 2BaO$	8.59×10^{-14}	550	0.0522	4.07×10^{-14}
110th	$12B + O_2 \leftrightharpoons 2B_6O$	8.49×10^{-14}	2390	0.0853	1.52×10^{-14}
111th	$2Mg + O_2 \leftrightharpoons 2MgO$	2.03×10^{-17}	2.26	0.198	8.91×10^{-15}
112th	$2Sr + O_2 \leftrightharpoons 2SrO$	2.08×10^{-17}	5.40	0.0772	1.48×10^{-15}
113th	$\frac{4}{3}Ce + O_2 \leftrightharpoons \frac{2}{3}Ce_2O_3$	3.12×10^{-17}	7	0.0615	1.37×10^{-15}
114th	$2Ti_6O + O_2 \leftrightharpoons 4Ti_3O$	3.08×10^{-17}	3.77	0.0313	1.28×10^{-15}
115th	$U + O_2 \leftrightharpoons UO_2$	3.14×10^{-16}	57.8	0.0420	1.14×10^{-15}

Continued on next page

Place	Transition	Probability of crossing	Price $/kg	Oxygen transfer capacity	Score
116th	$6Zr + O_2 \leftrightharpoons 2Zr_3O$	1.38×10^{-17}	23.1	0.0373	1.11×10^{-16}
117th	$4Li + O_2 \leftrightharpoons 2Li_2O$	9.19×10^{-18}	116	0.232	9.24×10^{-17}
118th	$Hf + O_2 \leftrightharpoons HfO_2$	1.92×10^{-16}	1410	0.0548	3.72×10^{-17}
119th	$\frac{4}{3}Pr + O_2 \leftrightharpoons \frac{2}{3}Pr_2O_3$	6.36×10^{-18}	85	0.0612	2.29×10^{-17}
120th	$2Be + O_2 \leftrightharpoons 2BeO$	1.03×10^{-17}	832	0.320	1.97×10^{-17}
121st	$\frac{4}{3}Nd + O_2 \leftrightharpoons \frac{2}{3}Nd_2O_3$	1.75×10^{-18}	60	0.0599	8.72×10^{-18}
122nd	$\frac{4}{3}Tb + O_2 \leftrightharpoons \frac{2}{3}Tb_2O_3$	1×10^{-17}	550	0.0549	5×10^{-18}
123rd	$\frac{4}{3}La + O_2 \leftrightharpoons \frac{2}{3}La_2O_3$	1.12×10^{-19}	7	0.0620	4.94×10^{-18}
124th	$\frac{4}{3}Sm + O_2 \leftrightharpoons \frac{2}{3}Sm_2O_3$	1.58×10^{-19}	14.4	0.0577	3.18×10^{-18}
125th	$2Ca + O_2 \leftrightharpoons 2CaO$	2.49×10^{-21}	5.93	0.143	2.99×10^{-19}
126th	$\frac{4}{3}Y + O_2 \leftrightharpoons \frac{2}{3}Y_2O_3$	5.81×10^{-21}	35	0.0915	7.60×10^{-20}
127th	$\frac{4}{3}Gd + O_2 \leftrightharpoons \frac{2}{3}Gd_2O_3$	9.47×10^{-21}	55	0.0554	4.77×10^{-20}
128th	$12Ti + O_2 \leftrightharpoons 2Ti_6O$	1.69×10^{-22}	3.77	0.0358	8.04×10^{-21}
129th	$Th + O_2 \leftrightharpoons ThO_2$	4.96×10^{-21}	176	0.0430	6.06×10^{-21}

Continued on next page

Place	Transition	Probability of crossing	Price $/kg	Oxygen transfer capacity	Score
130th	$\frac{4}{3}\mathrm{Dy} + \mathrm{O_2} \leftrightharpoons \frac{2}{3}\mathrm{Dy_2O_3}$	1.55×10^{-21}	350	0.0538	1.19×10^{-21}
131st	$\frac{4}{3}\mathrm{Er} + \mathrm{O_2} \leftrightharpoons \frac{2}{3}\mathrm{Er_2O_3}$	3.46×10^{-22}	95	0.0524	9.54×10^{-22}
132nd	$\frac{4}{3}\mathrm{Sc} + \mathrm{O_2} \leftrightharpoons \frac{2}{3}\mathrm{Sc_2O_3}$	5.96×10^{-21}	15 000	0.157	3.13×10^{-22}
133rd	$\frac{4}{3}\mathrm{Ho} + \mathrm{O_2} \leftrightharpoons \frac{2}{3}\mathrm{Ho_2O_3}$	7.15×10^{-22}	1400	0.0531	1.36×10^{-22}
134th	$\frac{4}{3}\mathrm{Tm} + \mathrm{O_2} \leftrightharpoons \frac{2}{3}\mathrm{Tm_2O_3}$	1.10×10^{-22}	6200	0.0519	4.60×10^{-24}
135th	$\frac{4}{3}\mathrm{Lu} + \mathrm{O_2} \leftrightharpoons \frac{2}{3}\mathrm{Lu_2O_3}$	4.12×10^{-23}	6270	0.0503	1.65×10^{-24}
136th	$2\mathrm{Eu} + \mathrm{O_2} \leftrightharpoons 2\mathrm{EuO}$	8.76×10^{-25}	258	0.0476	8.08×10^{-25}
137th	$2\mathrm{Yb} + \mathrm{O_2} \leftrightharpoons 2\mathrm{YbO}$	7.85×10^{-27}	1600	0.0423	1.04×10^{-27}
138th	$\frac{4}{3}\mathrm{TcO_2} + \mathrm{O_2} \leftrightharpoons \frac{2}{3}\mathrm{Tc_2O_7}$	0.494	—	0.0468	0
139th	$2\mathrm{Pu_2O_3} + \mathrm{O_2} \leftrightharpoons 4\mathrm{PuO_2}$	0.156	—	0.0103	0
140th	$\mathrm{Tc} + \mathrm{O_2} \leftrightharpoons \mathrm{TcO_2}$	0.0466	—	0.0936	0
141st	$\mathrm{Pa} + \mathrm{O_2} \leftrightharpoons \mathrm{PaO_2}$	2.49×10^{-10}	—	0.0432	0
142nd	$2\mathrm{Np_2O_3} + \mathrm{O_2} \leftrightharpoons 4\mathrm{NpO_2}$	1.13×10^{-10}	—	0.0105	0
143rd	$\mathrm{Np_2O} + \mathrm{O_2} \leftrightharpoons \mathrm{Np_2O_3}$	2.41×10^{-16}	—	0.0253	0

Continued on next page

Place	Transition	Probability of crossing	Price $/kg	Oxygen transfer capacity	Score
144^{th}	$4Np + O_2 \leftrightharpoons 2Np_2O$	1.41×10^{-17}	—	0.0211	0
145^{th}	$\frac{4}{5}Pu_3O_2 + O_2 \leftrightharpoons \frac{6}{5}Pu_2O_3$	1.10×10^{-17}	—	0.0205	0
146^{th}	$\frac{4}{3}Ac + O_2 \leftrightharpoons \frac{2}{3}Ac_2O_3$	5.71×10^{-18}	—	0.0395	0
147^{th}	$\frac{4}{3}Pm + O_2 \leftrightharpoons \frac{2}{3}Pm_2O_3$	3.30×10^{-19}	—	0.0596	0
148^{th}	$3Pu + O_2 \leftrightharpoons Pu_3O_2$	7.02×10^{-20}	—	0.0246	0

A.3 Ranking for filtered trimetallic CLOU transitions

The top 100 entries in the ranking of filtered mono-, bi- and trimetallic CLOU transitions.

Place	Transition	Probability of crossing	Price $/kg	Oxygen transfer capacity	Score
1st	$4Fe_3O_4 + O_2 \leftrightharpoons 6Fe_2O_3$	0.478	0.0800	0.0148	443
2nd	$6FeO + O_2 \leftrightharpoons 2Fe_3O_4$	0.0904	0.0800	0.0318	180
3rd	$\frac{4}{3}Fe_2SiO_4 + \frac{4}{3}FeSiO_3 + O_2 \leftrightharpoons 2Fe_2O_3 + \frac{8}{3}SiO_2$	0.442	0.812	0.0178	48.4
4th	$\frac{1}{7}Zn_3Cu + \frac{1}{14}Zn_8Cu_5 + O_2 \leftrightharpoons \frac{1}{2}Zn_2CuO_4$	0.547	3.85	0.0631	44.8
5th	$4Fe_2O_3 + 4FeSiO_3 + O_2 \leftrightharpoons 6Fe_2O_3 + 4SiO_2$	0.531	0.538	0.007 62	37.6
6th	$\frac{1}{2}MgO + \frac{1}{7}Zn_3Cu + \frac{1}{14}Zn_8Cu_5 + O_2 \leftrightharpoons \frac{1}{2}MgO + \frac{1}{2}Zn_2CuO_4$	0.536	3.46	0.0420	32.6
7th	$4Fe_3O_4 + 3NaFeO_2 + O_2 \leftrightharpoons 6Fe_2O_3 + 3NaFeO_2$	0.455	0.573	0.008 03	31.9
8th	$\frac{12}{5}Fe_2SiO_4 + \frac{6}{5}FeSiO_3 + O_2 \leftrightharpoons 2Fe_3O_4 + \frac{18}{5}SiO_2$	0.377	0.766	0.0129	31.8
9th	$\frac{3}{28}Zn_{13}Fe + \frac{11}{28}ZnFe_2O_4 + O_2 \leftrightharpoons \frac{25}{28}Zn_2FeO_4$	0.311	1.91	0.0373	30.4
10th	$\frac{8}{23}Cu_2O + \frac{8}{23}Zn_3Cu + O_2 \leftrightharpoons \frac{6}{23}Cu_2O + \frac{12}{23}Zn_2CuO_4$	0.519	4.37	0.0498	29.6

Continued on next page

Place	Transition	Probability of crossing	Price $/kg	Oxygen transfer capacity	Score
11th	$\frac{4}{37}Al_2O_3 + \frac{12}{37}AlCuO_2 + \frac{8}{37}Zn_5Cu + O_2 \leftrightharpoons \frac{10}{37}Al_2O_3 + \frac{20}{37}Zn_2CuO_4$	0.538	3.37	0.0362	29
12th	$4Fe_3O_4 + \frac{4}{3}Mn_3O_4 + O_2 \leftrightharpoons 6Fe_2O_3 + \frac{4}{3}Mn_3O_4$	0.460	0.575	0.006 42	25.7
13th	$2Fe + O_2 \leftrightharpoons 2FeO$	0.003 59	0.0800	0.111	25
14th	$4Fe_3O_4 + \frac{6}{5}SrFe_2O_4 + O_2 \leftrightharpoons 6Fe_2O_3 + \frac{6}{5}SrFe_2O_4$	0.462	0.489	0.005 23	24.6
15th	$4SiO_2 + 2Fe_2SiO_4 + O_2 \leftrightharpoons 2Fe_2O_3 + 6SiO_2$	0.497	1.18	0.0114	24.1
16th	$4Fe_3O_4 + \frac{60}{11}SiO_2 + O_2 \leftrightharpoons 6Fe_2O_3 + \frac{60}{11}SiO_2$	0.449	0.652	0.006 91	23.8
17th	$3Al_2O_3 + 4Fe_3O_4 + O_2 \leftrightharpoons 3Al_2O_3 + 6Fe_2O_3$	0.451	0.690	0.007 20	23.5
18th	$4Fe_3O_4 + 6MgO + O_2 \leftrightharpoons 6Fe_2O_3 + 6MgO$	0.455	0.807	0.007 92	22.4
19th	$\frac{14}{13}Fe_2O_3 + \frac{14}{13}Fe_2SiO_4 + \frac{14}{13}Mn_2SiO_4 + O_2 \leftrightharpoons \frac{28}{13}Fe_2O_3 + \frac{24}{13}SiO_2 + \frac{4}{13}Mn_7SiO_{12}$	0.485	1.03	0.009 20	21.6
20th	$4Fe_3O_4 + 6AlFeO_3 + O_2 \leftrightharpoons 6Fe_2O_3 + 6AlFeO_3$	0.430	0.538	0.005 40	21.6
21st	$4Fe_3O_4 + 6SiO_2 + O_2 \leftrightharpoons 6Fe_2O_3 + 6SiO_2$	0.446	0.690	0.006 67	21.6
22nd	$4Fe_3O_4 + 6FeSiO_3 + O_2 \leftrightharpoons 6Fe_2O_3 + 6FeSiO_3$	0.430	0.538	0.005 34	21.4

Continued on next page

Place	Transition	Probability of crossing	Price $/kg	Oxygen transfer capacity	Score
23rd	$\frac{4}{9}Zn_2CuO_4 + \frac{8}{9}ZnCu + O_2 \leftrightharpoons \frac{2}{9}Cu_2O + \frac{8}{9}Zn_2CuO_4$	0.540	4.15	0.0320	20.9
24th	$\frac{34}{63}Cu_2O + \frac{32}{63}Zn_5Cu + O_2 \leftrightharpoons \frac{40}{63}Zn_2CuO_4 + \frac{20}{63}Zn_4Cu_3$	0.503	4.01	0.0331	20.8
25th	$3SiO_2 + 3Fe_2SiO_4 + O_2 \leftrightharpoons 2Fe_3O_4 + 6SiO_2$	0.404	0.995	0.0100	20.3
26th	$\frac{8}{23}Cu_2O + \frac{24}{23}MgO + \frac{8}{23}Zn_3Cu + O_2 \leftrightharpoons \frac{6}{23}Cu_2O + \frac{24}{23}MgO + \frac{12}{23}Zn_2CuO_4$	0.495	3.66	0.0290	19.6
27th	$\frac{12}{5}Fe_3O_4 + 6FeSiO_3 + O_2 \leftrightharpoons \frac{22}{5}Fe_3O_4 + 6SiO_2$	0.388	0.652	0.006 56	19.5
28th	$\frac{10}{33}Al_2O_3 + \frac{4}{11}AlCuO_2 + \frac{4}{33}Zn_8Cu_5 + O_2 \leftrightharpoons \frac{8}{33}Al_2O_3 + \frac{16}{33}AlCuO_2 + \frac{16}{33}Zn_2CuO_4$	0.487	3.55	0.0284	19.5
29th	$\frac{10}{19}Cu_2O + \frac{16}{19}Zn_3Cu + O_2 \leftrightharpoons \frac{12}{19}Zn_2CuO_4 + \frac{24}{19}ZnCu$	0.508	4.15	0.0318	19.5
30th	$6SiO_2 + 2Fe_2SiO_4 + O_2 \leftrightharpoons 2Fe_2O_3 + 8SiO_2$	0.536	1.30	0.009 42	19.4
31st	$2Cu_2O + O_2 \leftrightharpoons 4CuO$	0.450	5.90	0.0503	19.2
32nd	$4Fe_3O_4 + \frac{36}{5}SiO_2 + O_2 \leftrightharpoons 6Fe_2O_3 + \frac{36}{5}SiO_2$	0.441	0.766	0.006 21	17.9

Continued on next page

Place	Transition	Probability of crossing	Price $/kg	Oxygen transfer capacity	Score
33rd	$\frac{25}{28}MgO + \frac{3}{28}Zn_{13}Fe + \frac{11}{28}ZnFe_2O_4 + O_2 \leftrightharpoons \frac{25}{28}MgO + \frac{25}{28}Zn_2FeO_4$	0.289	2	0.0246	17.8
34th	$4Mn_3O_4 + O_2 \leftrightharpoons 6Mn_2O_3$	0.485	2.06	0.0150	17.7
35th	$4Fe_3O_4 + \frac{2}{7}K_4Fe_2O_5 + O_2 \leftrightharpoons 6Fe_2O_3 + \frac{2}{7}K_4Fe_2O_5$	0.471	1.16	0.008 70	17.7
36th	$4Al_2O_3 + 4Fe_3O_4 + O_2 \leftrightharpoons 4Al_2O_3 + 6Fe_2O_3$	0.443	0.812	0.006 48	17.7
37th	$4Fe_3O_4 + 2Mn_3O_4 + O_2 \leftrightharpoons 6Fe_2O_3 + 2Mn_3O_4$	0.452	0.740	0.005 74	17.5
38th	$\frac{7}{8}FeSiO_3 + \frac{7}{8}Mn_2SiO_4 + \frac{7}{8}MnFeSiO_4 + O_2 \leftrightharpoons \frac{7}{8}Fe_2O_3 + \frac{9}{4}SiO_2 + \frac{3}{8}Mn_7SiO_{12}$	0.476	1.51	0.0111	17.5
39th	$\frac{25}{56}Al_2O_3 + \frac{3}{28}Zn_{13}Fe + \frac{11}{28}ZnFe_2O_4 + O_2 \leftrightharpoons \frac{25}{56}Al_2O_3 + \frac{25}{28}Zn_2FeO_4$	0.284	1.91	0.0230	17.1
40th	$\frac{1}{4}MnZn_5 + \frac{1}{4}Mn_2ZnO_4 + O_2 \leftrightharpoons \frac{3}{4}MnZn_2O_4$	0.193	2.57	0.0447	16.7
41st	$4Fe_3O_4 + 6NaFeO_2 + O_2 \leftrightharpoons 6Fe_2O_3 + 6NaFeO_2$	0.438	0.820	0.006 25	16.7
42nd	$\frac{3}{28}Zn_{13}Fe + \frac{69}{112}ZnFe_2O_4 + O_2 \leftrightharpoons \frac{25}{28}Zn_2FeO_4 + \frac{25}{112}ZnFe_2O_4$	0.193	1.73	0.0298	16.7

Continued on next page

Place	Transition	Probability of crossing	Price $/kg	Oxygen transfer capacity	Score
43rd	$2MgFe_2O_4 + 2Fe_2SiO_4 + 2MgSiO_3 + O_2 \leftrightharpoons 4Fe_2O_3 + 2SiO_2 + 2Mg_2SiO_4$	0.559	1.08	0.006 44	16.6
44th	$\frac{11}{56}Zn_{13}Fe + \frac{11}{28}ZnFe_2O_4 + O_2 \leftrightharpoons \frac{5}{56}Zn_{13}Fe + \frac{25}{28}Zn_2FeO_4$	0.227	2.14	0.0311	16.4
45th	$\frac{66}{35}CaO + \frac{44}{35}Mn_3O_4 + O_2 \leftrightharpoons \frac{6}{7}Ca_2Mn_3O_8 + \frac{6}{35}CaMn_7O_{12}$	0.554	3.35	0.0198	16.3
46th	$2Fe_3O_4 + 6FeSiO_3 + O_2 \leftrightharpoons 4Fe_3O_4 + 6SiO_2$	0.324	0.690	0.006 96	16.3
47th	$2Fe_3O_4 + 6Fe_2SiO_4 + O_2 \leftrightharpoons 4Fe_3O_4 + 6FeSiO_3$	0.308	0.538	0.005 52	15.8
48th	$\frac{8}{23}Cu_2O + \frac{48}{23}MgO + \frac{8}{23}Zn_3Cu + O_2 \leftrightharpoons \frac{6}{23}Cu_2O + \frac{48}{23}MgO + \frac{12}{23}Zn_2CuO_4$	0.476	3.31	0.0220	15.8
49th	$\frac{1}{7}Zn_3Cu + \frac{1}{14}Zn_8Cu_5 + \frac{1}{14}Sr_9Zn_4Cu_2O_{14} + O_2 \leftrightharpoons \frac{1}{2}Zn_2CuO_4 + \frac{1}{14}Sr_9Zn_4Cu_2O_{14}$	0.525	4.24	0.0247	15.3
50th	$\frac{38}{33}Cu_2O + \frac{4}{33}Zn_8Cu_5 + O_2 \leftrightharpoons \frac{40}{33}Cu_2O + \frac{16}{33}Zn_2CuO_4$	0.488	5.13	0.0314	14.9
51st	$NaCrO_2 + \frac{1}{2}Na_4CrO_4 + O_2 \leftrightharpoons \frac{3}{2}Na_2CrO_4$	0.407	4.57	0.0335	14.9
52nd	$4Cu + O_2 \leftrightharpoons 2Cu_2O$	0.262	5.90	0.0670	14.9

Continued on next page

Place	Transition	Probability of crossing	Price $/kg	Oxygen transfer capacity	Score
53rd	$\frac{4}{3}Al_2SiO_5 + \frac{4}{3}Fe_2SiO_4 + \frac{4}{3}FeSiO_3 + O_2 \leftrightharpoons 2Fe_2O_3 + \frac{8}{3}SiO_2 + \frac{4}{3}Al_2SiO_5$	0.408	1.22	0.008 80	14.7
54th	$\frac{7}{3}SiO_2 + \frac{7}{3}Mn_2SiO_4 + O_2 \leftrightharpoons 4SiO_2 + \frac{2}{3}Mn_7SiO_{12}$	0.452	1.99	0.0128	14.5
55th	$\frac{16}{23}Al_2O_3 + \frac{16}{23}AlCuO_2 + \frac{8}{23}Zn_3Cu + O_2 \leftrightharpoons \frac{18}{23}Al_2O_3 + \frac{12}{23}AlCuO_2 + \frac{12}{23}Zn_2CuO_4$	0.473	3.14	0.0193	14.5
56th	$\frac{2}{3}Cu_2O + \frac{32}{33}MgO + \frac{4}{33}Zn_8Cu_5 + O_2 \leftrightharpoons \frac{8}{11}Cu_2O + \frac{32}{33}MgO + \frac{16}{33}Zn_2CuO_4$	0.481	4.22	0.0252	14.3
57th	$8SiO_2 + 4FeSiO_3 + O_2 \leftrightharpoons 2Fe_2O_3 + 12SiO_2$	0.574	1.45	0.006 96	13.8
58th	$\frac{1}{4}Ce_2O_3 + \frac{1}{7}Zn_3Cu + \frac{1}{14}Zn_8Cu_5 + O_2 \leftrightharpoons \frac{1}{4}Ce_2O_3 + \frac{1}{2}Zn_2CuO_4$	0.533	4.64	0.0236	13.6
59th	$2Cu_2O + \frac{4}{3}MgO + O_2 \leftrightharpoons 4CuO + \frac{4}{3}MgO$	0.467	4.99	0.0289	13.5

Continued on next page

Place	Transition	Probability of crossing	Price $/kg	Oxygen transfer capacity	Score
60th	$\frac{10}{11}Cu_2O + \frac{16}{33}MgO + \frac{4}{33}Zn_8Cu_5 + O_2 \leftrightharpoons \frac{32}{33}Cu_2O + \frac{16}{33}MgO + \frac{16}{33}Zn_2CuO_4$	0.485	4.68	0.0260	13.5
61st	$\frac{3}{28}Zn_{13}Fe + \frac{3}{4}ZnFe_2O_4 + O_2 \leftrightharpoons \frac{25}{28}Zn_2FeO_4 + \frac{5}{14}ZnFe_2O_4$	0.161	1.65	0.0266	13
62nd	$2Cu_2O + 2MgO + O_2 \leftrightharpoons 4CuO + 2MgO$	0.474	4.69	0.0257	13
63rd	$\frac{25}{28}Al_2O_3 + \frac{3}{28}Zn_{13}Fe + \frac{11}{28}ZnFe_2O_4 + O_2 \leftrightharpoons \frac{25}{28}Al_2O_3 + \frac{25}{28}Zn_2FeO_4$	0.265	1.91	0.0182	12.6
64th	$4Fe_3O_4 + 8NaFeO_2 + O_2 \leftrightharpoons 6Fe_2O_3 + 8NaFeO_2$	0.428	0.926	0.005 44	12.6
65th	$\frac{4}{11}SbO_2 + \frac{2}{11}CuSbO_3 + \frac{4}{11}Zn_3Cu + O_2 \leftrightharpoons \frac{6}{11}SbO_2 + \frac{6}{11}Zn_2CuO_4$	0.532	4.65	0.0220	12.6
66th	$\frac{8}{3}NaCrO_2 + O_2 \leftrightharpoons \frac{2}{3}Cr_2O_3 + \frac{4}{3}Na_2CrO_4$	0.481	5.34	0.0278	12.5
67th	$Al_2O_3 + 6FeO + O_2 \leftrightharpoons Al_2O_3 + 2Fe_3O_4$	0.0787	0.538	0.0170	12.5
68th	$2Cu_2O + \frac{4}{11}MgCu_2O_3 + O_2 \leftrightharpoons 4CuO + \frac{4}{11}MgCu_2O_3$	0.464	5.64	0.0303	12.5

Continued on next page

Place	Transition	Probability of crossing	Price $/kg	Oxygen transfer capacity	Score
69th	$\frac{8}{23}Cu_2O + \frac{24}{23}AlCuO_2 + \frac{8}{23}Zn_3Cu + O_2 \leftrightharpoons \frac{6}{23}Cu_2O + \frac{24}{23}AlCuO_2 + \frac{12}{23}Zn_2CuO_4$	0.476	4.14	0.0216	12.4
70th	$2Cu_2O + \frac{16}{15}SiO_2 + O_2 \leftrightharpoons 4CuO + \frac{16}{15}SiO_2$	0.470	5.06	0.0265	12.3
71st	$6NaMnO_2 + O_2 \leftrightharpoons 2Na_2MnO_3 + 2NaMn_2O_4$	0.479	2.55	0.0131	12.3
72nd	$\frac{35}{6}SiO_2 + \frac{7}{3}Mn_2SiO_4 + O_2 \leftrightharpoons \frac{15}{2}SiO_2 + \frac{2}{3}Mn_7SiO_{12}$	0.533	1.96	0.009 02	12.2
73rd	$4Fe_3O_4 + \frac{12}{5}Ti_2FeO_5 + O_2 \leftrightharpoons 6Fe_2O_3 + \frac{12}{5}Ti_2FeO_5$	0.444	1.00	0.005 43	12
74th	$Zn_2CuO_4 + \frac{1}{2}Zn_4Cu_3 + O_2 \leftrightharpoons \frac{3}{2}Zn_2CuO_4 + ZnCu$	0.544	4.01	0.0177	12
75th	$2Cu_2O + \frac{4}{3}SiO_2 + O_2 \leftrightharpoons 4CuO + \frac{4}{3}SiO_2$	0.474	4.90	0.0248	12
76th	$\frac{4}{3}Zn_2CuO_4 + \frac{8}{9}ZnCu + O_2 \leftrightharpoons \frac{2}{9}Cu_2O + \frac{16}{9}Zn_2CuO_4$	0.558	4.01	0.0168	11.7
77th	$6Al_2O_3 + 4Fe_3O_4 + O_2 \leftrightharpoons 6Al_2O_3 + 6Fe_2O_3$	0.430	0.995	0.005 40	11.7
78th	$2Cu_2O + 4MgO + O_2 \leftrightharpoons 4CuO + 4MgO$	0.489	4.08	0.0193	11.5
79th	$4Fe_3O_4 + \frac{8}{5}LaFeO_3 + O_2 \leftrightharpoons 6Fe_2O_3 + \frac{8}{5}LaFeO_3$	0.462	0.808	0.004 00	11.4

Continued on next page

Place	Transition	Probability of crossing	Price $/kg	Oxygen transfer capacity	Score
80th	$7SiO_2 + \frac{7}{3}Mn_2SiO_4 + O_2 \leftrightharpoons \frac{26}{3}SiO_2 + \frac{2}{3}Mn_7SiO_{12}$	0.544	1.96	0.008 22	11.4
81st	$4Fe_3O_4 + \frac{8}{5}CeFeO_3 + O_2 \leftrightharpoons 6Fe_2O_3 + \frac{8}{5}CeFeO_3$	0.462	0.808	0.003 97	11.4
82nd	$Mn_3O_4 + 6NaMnO_2 + O_2 \leftrightharpoons 3NaMnO_2 + 3NaMn_2O_4$	0.537	2.45	0.0103	11.3
83rd	$6FeO + \frac{3}{2}NaFeO_2 + O_2 \leftrightharpoons 2Fe_3O_4 + \frac{3}{2}NaFeO_2$	0.0768	0.573	0.0169	11.3
84th	$2Al_2O_3 + 4MnAl_2O_4 + O_2 \leftrightharpoons 6Al_2O_3 + 2Mn_2O_3$	0.536	1.95	0.008 17	11.2
85th	$\frac{14}{3}MnSiO_3 + \frac{7}{12}Mn_7SiO_{12} + O_2 \leftrightharpoons 4SiO_2 + \frac{5}{4}Mn_7SiO_{12}$	0.505	2.00	0.008 73	11
86th	$\frac{8}{23}Cu_2O + \frac{24}{23}CaZnO_2 + \frac{8}{23}Zn_3Cu + O_2 \leftrightharpoons \frac{6}{23}Cu_2O + \frac{24}{23}CaZnO_2 + \frac{12}{23}Zn_2CuO_4$	0.476	4.37	0.0201	10.9
87th	$\frac{3}{2}MgO + NaCrO_2 + \frac{1}{2}Na_4CrO_4 + O_2 \leftrightharpoons \frac{3}{2}MgO + \frac{3}{2}Na_2CrO_4$	0.424	4.00	0.0206	10.9
88th	$\frac{22}{17}Mn_2O_3 + \frac{44}{17}NaMnO_2 + O_2 \leftrightharpoons \frac{20}{17}Na_2Mn_3O_7 + \frac{4}{17}NaMn_7O_{12}$	0.287	2.39	0.0181	10.9
89th	$2Cu_2O + 2Fe_2O_3 + O_2 \leftrightharpoons 4CuO + 2Fe_2O_3$	0.494	2.99	0.0131	10.8

Continued on next page

Place	Transition	Probability of crossing	Price $/kg	Oxygen transfer capacity	Score
90th	$\frac{68}{161}Cu_2O + \frac{8}{23}Zn_3Cu + \frac{12}{161}Sr_9Zn_4Cu_2O_{14} + O_2 \leftrightharpoons \frac{54}{161}Cu_2O + \frac{12}{23}Zn_2CuO_4 + \frac{12}{161}Sr_9Zn_4Cu_2O_{14}$	0.490	4.57	0.0202	10.8
91st	$\frac{4}{3}Ti_2FeO_5 + \frac{8}{3}TiFeO_3 + O_2 \leftrightharpoons \frac{10}{3}TiO_2 + 2TiFe_2O_5$	0.460	2.19	0.0103	10.8
92nd	$\frac{8}{3}Mn_2O_3 + \frac{8}{3}NaMnO_2 + O_2 \leftrightharpoons 2Mn_2O_3 + \frac{4}{3}Na_2Mn_3O_7$	0.378	2.31	0.0131	10.7
93rd	$2Cu_2O + \frac{16}{3}MgO + O_2 \leftrightharpoons 4CuO + \frac{16}{3}MgO$	0.496	3.82	0.0165	10.7
94th	$2Al_2O_3 + 2Al_2SiO_5 + 2Fe_2SiO_4 + O_2 \leftrightharpoons 4Al_2O_3 + 2Fe_2O_3 + 4SiO_2$	0.516	1.45	0.006 00	10.7
95th	$2Cu_2O + \frac{4}{3}AlCuO_2 + O_2 \leftrightharpoons 4CuO + \frac{4}{3}AlCuO_2$	0.479	5.10	0.0225	10.6
96th	$2Al_2O_3 + 2Cu_2O + O_2 \leftrightharpoons 2Al_2O_3 + 4CuO$	0.494	3.91	0.0167	10.6
97th	$\frac{4}{3}Fe_2SiO_4 + \frac{4}{3}FeSiO_3 + \frac{4}{3}Ti_2FeO_5 + O_2 \leftrightharpoons 2Fe_2O_3 + \frac{8}{3}SiO_2 + \frac{4}{3}Ti_2FeO_5$	0.408	1.46	0.007 55	10.5
98th	$4Cu + \frac{4}{13}MgO + O_2 \leftrightharpoons 2Cu_2O + \frac{4}{13}MgO$	0.254	5.64	0.0466	10.5

Continued on next page

Place	Transition	Probability of crossing	Price $/kg	Oxygen transfer capacity	Score
99$^{\text{th}}$	$\frac{3}{4}Al_2O_3 + NaCrO_2 + \frac{1}{2}Na_4CrO_4 + O_2 \leftrightharpoons \frac{3}{4}Al_2O_3 + \frac{3}{2}Na_2CrO_4$	0.428	3.91	0.0190	10.4
100$^{\text{th}}$	$2Cu_2O + 6MgO + O_2 \leftrightharpoons 4CuO + 6MgO$	0.499	3.72	0.0154	10.3

A.4 Ranking for unfiltered bimetallic CLOU transitions

The top 100 entries in the ranking of unfiltered mono- and bimetallic CLOU transitions.

Place	Transition	Probability of crossing	Price \$/kg	Oxygen transfer capacity	Score
1st	$\frac{1}{2}FeS_2 + O_2 \leftrightharpoons \frac{1}{6}FeS_3 + \frac{1}{6}Fe_2S_3O_{12}$	0.273	0.0933	0.0880	1.29×10^3
2nd	$\frac{1}{4}FeS_2 + \frac{1}{4}FeSO_4 + O_2 \leftrightharpoons \frac{1}{4}Fe_2S_3O_{12}$	0.306	0.0920	0.0725	1.21×10^3
3rd	$\frac{1}{10}Fe_3O_4 + \frac{3}{10}FeS_2 + O_2 \leftrightharpoons \frac{3}{5}FeSO_4$	0.149	0.0900	0.0855	707
4th	$\frac{1}{14}Fe_3O_4 + \frac{2}{7}FeS_2 + O_2 \leftrightharpoons \frac{1}{14}Fe_2S_3O_{12} + \frac{5}{14}FeSO_4$	0.120	0.0907	0.0917	608
5th	$\frac{1}{4}FeS_2 + \frac{1}{2}FeSO_4 + O_2 \leftrightharpoons \frac{1}{4}Fe_2S_3O_{12} + \frac{1}{4}FeSO_4$	0.205	0.0914	0.0536	600
6th	$4Fe_3O_4 + O_2 \leftrightharpoons 6Fe_2O_3$	0.478	0.0800	0.0148	443
7th	$\frac{1}{10}Fe_3O_4 + \frac{3}{5}FeS_2 + O_2 \leftrightharpoons \frac{3}{10}FeS_2 + \frac{3}{5}FeSO_4$	0.104	0.0914	0.0684	390
8th	$4FeSO_4 + O_2 \leftrightharpoons \frac{2}{3}Fe_2O_3 + \frac{4}{3}Fe_2S_3O_{12}$	0.527	0.0900	0.0118	347
9th	$\frac{3}{10}Fe_3O_4 + \frac{3}{10}FeS_2 + O_2 \leftrightharpoons \frac{1}{5}Fe_3O_4 + \frac{3}{5}FeSO_4$	0.0968	0.0867	0.0616	344
10th	$\frac{6}{5}FeO + \frac{6}{25}FeS_2 + O_2 \leftrightharpoons \frac{8}{25}Fe_3O_4 + \frac{12}{25}FeSO_4$	0.0786	0.0850	0.0601	278

Continued on next page

Place	Transition	Probability of crossing	Price $/kg	Oxygen transfer capacity	Score
11th	$\frac{1}{10}Fe_3O_4 + \frac{9}{10}FeS_2 + O_2 \leftrightharpoons \frac{3}{5}FeS_2 + \frac{3}{5}FeSO_4$	0.0858	0.0920	0.0570	266
12th	$2Fe_2O_3 + 4FeSO_4 + O_2 \leftrightharpoons \frac{8}{3}Fe_2O_3 + \frac{4}{3}Fe_2S_3O_{12}$	0.404	0.0867	0.008 55	199
13th	$6FeO + O_2 \leftrightharpoons 2Fe_3O_4$	0.0904	0.0800	0.0318	180
14th	$\frac{1}{6}As_2S_3 + O_2 \leftrightharpoons \frac{1}{6}As_2S_3O_{12}$	0.294	0.756	0.0918	178
15th	$\frac{1}{6}As_2S_3 + \frac{1}{6}AsS_3 + O_2 \leftrightharpoons \frac{1}{6}AsS_3 + \frac{1}{6}As_2S_3O_{12}$	0.269	0.647	0.0743	155
16th	$4Fe_2O_3 + 4FeSO_4 + O_2 \leftrightharpoons \frac{14}{3}Fe_2O_3 + \frac{4}{3}Fe_2S_3O_{12}$	0.354	0.0850	0.006 69	139
17th	$\frac{1}{3}MnN_2 + O_2 \leftrightharpoons \frac{1}{3}MnN_2O_6$	0.554	2.53	0.126	137
18th	$\frac{1}{6}As_2S_3 + \frac{1}{18}As_2SO_6 + O_2 \leftrightharpoons \frac{1}{6}As_2S_3O_{12} + \frac{1}{18}As_2SO_6$	0.274	0.829	0.0781	129
19th	$\frac{4}{109}Mn_3O_4 + \frac{36}{109}MnN_2 + O_2 \leftrightharpoons \frac{6}{109}Mn_2O_3 + \frac{36}{109}MnN_2O_6$	0.553	2.49	0.116	129
20th	$\frac{2}{5}Na_2O + \frac{2}{5}NaN_3 + O_2 \leftrightharpoons \frac{6}{5}NaNO_2$	0.539	2.91	0.126	117
21st	$4Fe_3O_4 + 6FeSO_4 + O_2 \leftrightharpoons 6Fe_2O_3 + 6FeSO_4$	0.424	0.0850	0.004 67	116
22nd	$\frac{1}{9}Mn_3O_4 + \frac{1}{3}MnN_2 + O_2 \leftrightharpoons \frac{1}{9}Mn_3O_4 + \frac{1}{3}MnN_2O_6$	0.551	2.42	0.0997	114

Continued on next page

Place	Transition	Probability of crossing	Price $/kg	Oxygen transfer capacity	Score
23rd	$\frac{2}{7}CdS_2 + O_2$	0.235	0.727	0.0698	113
	$\leftrightharpoons \frac{2}{7}CdS_2O_7$				
24th	$\frac{1}{6}As_2S_3 + \frac{1}{10}As_2SO_6 + O_2$	0.262	0.872	0.0697	105
	$\leftrightharpoons \frac{1}{6}As_2S_3O_{12} + \frac{1}{10}As_2SO_6$				
25th	$2AlN + O_2$	0.521	2.34	0.0936	104
	$\leftrightharpoons \frac{2}{3}Al_2O_3 + \frac{2}{3}AlN_3$				
26th	$ZnS_2 + O_2$	0.359	1.01	0.0564	100
	$\leftrightharpoons \frac{1}{2}ZnS_3 + \frac{1}{2}ZnSO_4$				
27th	$3SiS_2 + O_2$	0.360	0.703	0.0382	97.8
	$\leftrightharpoons SiO_2 + 2SiS_3$				
28th	$\frac{2}{9}Mn_3O_4 + \frac{1}{3}MnN_2 + O_2$	0.547	2.34	0.0827	96.4
	$\leftrightharpoons \frac{2}{9}Mn_3O_4 + \frac{1}{3}MnN_2O_6$				
29th	$\frac{1}{4}CaO + \frac{1}{8}CaN_6 + O_2$	0.526	3.82	0.135	93
	$\leftrightharpoons \frac{3}{8}CaN_2O_6$				
30th	$\frac{7}{10}Na_2O + \frac{2}{5}NaN_3 + O_2$	0.494	2.93	0.106	89.3
	$\leftrightharpoons \frac{3}{10}Na_2O + \frac{6}{5}NaNO_2$				
31st	$3FeS + 3FeS_2 + O_2$	0.0851	0.0920	0.0181	83.8
	$\leftrightharpoons \frac{1}{2}Fe_3O_4 + \frac{9}{2}FeS_2$				
32nd	$\frac{3}{8}CaO + \frac{1}{8}CaN_6 + O_2$	0.536	4.03	0.126	83.6
	$\leftrightharpoons \frac{1}{8}CaO + \frac{3}{8}CaN_2O_6$				
33rd	$\frac{1}{3}Mn_3O_4 + \frac{1}{3}MnN_2 + O_2$	0.542	2.30	0.0706	83.4
	$\leftrightharpoons \frac{1}{3}Mn_3O_4 + \frac{1}{3}MnN_2O_6$				
34th	$\frac{1}{4}CaO + \frac{1}{4}CaN_6 + O_2$	0.546	3.56	0.107	82.4
	$\leftrightharpoons \frac{1}{8}CaN_6 + \frac{3}{8}CaN_2O_6$				

Continued on next page

Place	Transition	Probability of crossing	Price $/kg	Oxygen transfer capacity	Score
35th	$\frac{1}{6}As_2S_3 + \frac{1}{6}As_2SO_6 + O_2 \leftrightharpoons \frac{1}{6}As_2S_3O_{12} + \frac{1}{6}As_2SO_6$	0.247	0.920	0.0600	80.7
36th	$3FeS + \frac{3}{2}FeS_2 + O_2 \leftrightharpoons \frac{1}{2}Fe_3O_4 + 3FeS_2$	0.0584	0.0914	0.0246	78.7
37th	$\frac{1}{6}As_2O_3 + \frac{1}{6}As_2S_3 + O_2 \leftrightharpoons \frac{1}{12}As_2S_3O_{12} + \frac{1}{4}As_2SO_6$	0.222	1.04	0.0710	75.9
38th	$CuS_2 + O_2 \leftrightharpoons \frac{1}{2}CuS_3 + \frac{1}{2}CuSO_4$	0.534	2.03	0.0573	75.4
39th	$\frac{1}{2}ZnS + O_2 \leftrightharpoons \frac{1}{2}ZnSO_4$	0.230	1.47	0.0940	73.7
40th	$2AlN + \frac{2}{3}AlN_3 + O_2 \leftrightharpoons \frac{2}{3}Al_2O_3 + \frac{4}{3}AlN_3$	0.550	2.43	0.0648	73.5
41st	$\frac{1}{2}ZnS + \frac{1}{28}ZnS_2 + O_2 \leftrightharpoons \frac{1}{28}ZnS_2 + \frac{1}{2}ZnSO_4$	0.226	1.42	0.0908	72.2
42nd	$4Fe_3O_4 + \frac{12}{7}FeN + O_2 \leftrightharpoons 6Fe_2O_3 + \frac{12}{7}FeN$	0.471	0.379	0.0111	69.3
43rd	$\frac{5}{8}CaO + \frac{1}{8}CaN_6 + O_2 \leftrightharpoons \frac{3}{8}CaO + \frac{3}{8}CaN_2O_6$	0.543	4.35	0.111	69.1
44th	$6FeO + 2FeS_2 + O_2 \leftrightharpoons 2Fe_3O_4 + 2FeS_2$	0.0768	0.0867	0.0154	68.3
45th	$4Fe_3O_4 + 12FeSO_4 + O_2 \leftrightharpoons 6Fe_2O_3 + 12FeSO_4$	0.391	0.0867	0.003 02	68.2
46th	$\frac{1}{2}CdS + O_2 \leftrightharpoons \frac{1}{2}CdSO_4$	0.207	1.04	0.0665	66.2

Continued on next page

Place	Transition	Probability of crossing	Price $/kg	Oxygen transfer capacity	Score
47th	$\frac{5}{9}Mn_3O_4 + \frac{1}{3}MnN_2 + O_2 \leftrightharpoons \frac{5}{9}Mn_3O_4 + \frac{1}{3}MnN_2O_6$	0.533	2.24	0.0547	65.2
48th	$\frac{4}{3}Fe_2O_3 + \frac{8}{3}FeN + O_2 \leftrightharpoons 2Fe_2O_3 + \frac{4}{3}FeN_2$	0.469	0.977	0.0266	63.9
49th	$Al_2O_3 + 2AlN + O_2 \leftrightharpoons \frac{5}{3}Al_2O_3 + \frac{2}{3}AlN_3$	0.546	2.20	0.0510	63.5
50th	$MnS_2 + O_2 \leftrightharpoons \frac{1}{2}MnS_3 + \frac{1}{2}MnSO_4$	0.152	0.753	0.0621	62.6
51st	$\frac{28}{15}Fe_2O_3 + \frac{8}{3}FeN + O_2 \leftrightharpoons \frac{38}{15}Fe_2O_3 + \frac{4}{3}FeN_2$	0.487	0.871	0.0224	62.4
52nd	$2Na_2O + O_2 \leftrightharpoons 4NaO$	0.367	3.04	0.103	61.9
53rd	$\frac{1}{3}NiN_2 + O_2 \leftrightharpoons \frac{1}{3}NiN_2O_6$	0.505	4.91	0.120	61.8
54th	$As_2O_3 + O_2 \leftrightharpoons As_2O_5$	0.427	1.74	0.0503	61.7
55th	$\frac{1}{4}SrO + \frac{1}{8}SrN_6 + O_2 \leftrightharpoons \frac{3}{8}SrN_2O_6$	0.557	3.65	0.0806	61.5
56th	$\frac{8}{3}Fe_2O_3 + \frac{8}{3}FeN + O_2 \leftrightharpoons \frac{10}{3}Fe_2O_3 + \frac{4}{3}FeN_2$	0.503	0.753	0.0180	60.3
57th	$\frac{1}{3}As_2O_3 + \frac{1}{6}As_2S_3 + O_2 \leftrightharpoons \frac{1}{3}As_2O_3 + \frac{1}{6}As_2S_3O_{12}$	0.244	1.19	0.0578	59.1
58th	$\frac{29}{32}CaO + \frac{1}{8}CaN_6 + O_2 \leftrightharpoons \frac{21}{32}CaO + \frac{3}{8}CaN_2O_6$	0.547	4.60	0.0974	57.9

Continued on next page

Place	Transition	Probability of crossing	Price $/kg	Oxygen transfer capacity	Score
59th	$4Fe_2O_3 + \frac{8}{3}FeN + O_2 \leftrightharpoons \frac{14}{3}Fe_2O_3 + \frac{4}{3}FeN_2$	0.520	0.618	0.0136	57.4
60th	$2NaNO_2 + O_2 \leftrightharpoons 2NaNO_3$	0.540	2.91	0.0604	56.1
61st	$CaO + \frac{1}{8}CaN_6 + O_2 \leftrightharpoons \frac{3}{4}CaO + \frac{3}{8}CaN_2O_6$	0.547	4.67	0.0937	54.9
62nd	$\frac{1}{8}Na_2S_5 + \frac{3}{8}Na_2SO_4 + O_2 \leftrightharpoons \frac{1}{2}Na_2S_2O_7$	0.207	1.57	0.0819	53.9
63rd	$As_2O_3 + \frac{7}{6}Fe_2O_3 + O_2 \leftrightharpoons \frac{1}{6}Fe_4As_2O_{11} + \frac{5}{3}FeAsO_4$	0.537	0.846	0.0170	53.9
64th	$\frac{7}{9}Mn_3O_4 + \frac{1}{3}MnN_2 + O_2 \leftrightharpoons \frac{7}{9}Mn_3O_4 + \frac{1}{3}MnN_2O_6$	0.525	2.20	0.0446	53.2
65th	$\frac{8}{7}Na_2S_5 + O_2 \leftrightharpoons \frac{12}{7}NaS_3 + \frac{2}{7}Na_2S_2O_7$	0.221	0.940	0.0450	52.9
66th	$\frac{1}{4}SrO + \frac{1}{4}SrN_6 + O_2 \leftrightharpoons \frac{1}{8}SrN_6 + \frac{3}{8}SrN_2O_6$	0.545	3.43	0.0640	50.9
67th	$8FeO + 4FeS + O_2 \leftrightharpoons 10FeO + 2FeS_2$	0.0716	0.0850	0.0118	49.9
68th	$\frac{28}{3}Fe_2O_3 + \frac{8}{3}FeN + O_2 \leftrightharpoons 10Fe_2O_3 + \frac{4}{3}FeN_2$	0.547	0.379	0.006 90	49.8
69th	$\frac{1}{4}ZnO + \frac{1}{2}ZnS + O_2 \leftrightharpoons \frac{1}{4}ZnO + \frac{1}{2}ZnSO_4$	0.214	1.74	0.0806	49.5
70th	$4FeO + 4FeS + O_2 \leftrightharpoons 6FeO + 2FeS_2$	0.0495	0.0867	0.0171	48.9

Continued on next page

Place	Transition	Probability of crossing	Price $/kg	Oxygen transfer capacity	Score
71st	$\frac{1}{4}CuO + \frac{1}{8}CuN_6 + O_2 \leftrightharpoons \frac{3}{8}CuN_2O_6$	0.365	3.81	0.101	48.6
72nd	$\frac{4}{3}Fe_2SiO_4 + \frac{4}{3}FeSiO_3 + O_2 \leftrightharpoons 2Fe_2O_3 + \frac{8}{3}SiO_2$	0.442	0.812	0.0178	48.4
73rd	$\frac{2}{7}CdS_2 + \frac{2}{7}CdSO_4 + O_2 \leftrightharpoons \frac{2}{7}CdS_2O_7 + \frac{2}{7}CdSO_4$	0.189	0.852	0.0436	48.4
74th	$\frac{1}{4}CuO + \frac{1}{4}CuN_6 + O_2 \leftrightharpoons \frac{1}{8}CuN_6 + \frac{3}{8}CuN_2O_6$	0.424	3.55	0.0805	48
75th	$\frac{1}{2}Na_2O + 2NaNO_2 + O_2 \leftrightharpoons \frac{1}{2}Na_2O + 2NaNO_3$	0.535	2.93	0.0525	47.9
76th	$\frac{10}{11}As_2O_3 + \frac{10}{11}Fe_3O_4 + O_2 \leftrightharpoons \frac{4}{11}Fe_4As_2O_{11} + \frac{2}{11}Fe_7As_6O_{24}$	0.411	0.744	0.0169	46.7
77th	$\frac{1}{4}CuS_2 + \frac{1}{4}Cu_2SO_4 + O_2 \leftrightharpoons \frac{3}{4}CuSO_4$	0.435	3	0.0637	46.1
78th	$\frac{11}{8}CaO + \frac{1}{8}CaN_6 + O_2 \leftrightharpoons \frac{9}{8}CaO + \frac{3}{8}CaN_2O_6$	0.548	4.88	0.0812	45.6
79th	$\frac{3}{8}CuO + \frac{1}{8}CuN_6 + O_2 \leftrightharpoons \frac{1}{8}CuO + \frac{3}{8}CuN_2O_6$	0.388	4.02	0.0944	45.5
80th	$\frac{12}{13}As_2O_3 + \frac{16}{13}Fe_3O_4 + O_2 \leftrightharpoons \frac{10}{13}Fe_2O_3 + \frac{4}{13}Fe_7As_6O_{24}$	0.400	0.633	0.0143	45.2
81st	$\frac{1}{5}VN_3 + O_2 \leftrightharpoons \frac{1}{5}VN_3O_{10}$	0.493	7.73	0.141	45
82nd	$3FeN + O_2 \leftrightharpoons \frac{1}{2}Fe_3O_4 + \frac{3}{2}FeN_2$	0.273	1.43	0.0466	44.6

Continued on next page

Place	Transition	Probability of crossing	Price $/kg	Oxygen transfer capacity	Score
83rd	$\frac{5}{8}SrO + \frac{1}{8}SrN_6 + O_2 \leftrightharpoons \frac{3}{8}SrO + \frac{3}{8}SrN_2O_6$	0.550	4.09	0.0659	44.4
84th	$\frac{1}{2}CdS + \frac{1}{2}CdS_2 + O_2 \leftrightharpoons \frac{1}{2}CdS_2 + \frac{1}{2}CdSO_4$	0.171	0.852	0.0443	44.4
85th	$MnS_2 + MnSO_4 + O_2 \leftrightharpoons \frac{1}{2}MnS_3 + \frac{3}{2}MnSO_4$	0.278	0.884	0.0282	44.4
86th	$2AlN + 2AlN_3 + O_2 \leftrightharpoons \frac{2}{3}Al_2O_3 + \frac{8}{3}AlN_3$	0.547	2.48	0.0401	44.2
87th	$2Al_2O_3 + 2AlN + O_2 \leftrightharpoons \frac{8}{3}Al_2O_3 + \frac{2}{3}AlN_3$	0.535	2.13	0.0351	44.2
88th	$\frac{1}{2}CuS + \frac{1}{2}CuS_2 + O_2 \leftrightharpoons \frac{1}{2}CuS_2 + \frac{1}{2}CuSO_4$	0.334	2.42	0.0637	44
89th	$\frac{1}{2}KN_3 + O_2 \leftrightharpoons \frac{1}{2}KN_3O_4$	0.397	5.33	0.116	43.1
90th	$As_2O_3 + \frac{1}{13}AsN_9 + O_2 \leftrightharpoons As_2O_5 + \frac{1}{13}AsN_9$	0.434	2.00	0.0393	42.6
91st	$\frac{1}{3}NiO + \frac{1}{3}NiN_2 + O_2 \leftrightharpoons \frac{1}{3}NiO + \frac{1}{3}NiN_2O_6$	0.517	5.98	0.0984	42.5
92nd	$As_2O_3 + \frac{1}{4}AsCl_3 + O_2 \leftrightharpoons As_2O_5 + \frac{1}{4}AsCl_3$	0.436	1.68	0.0317	41.1
93rd	$\frac{4}{11}TiO_2 + \frac{2}{11}TiS_3 + O_2 \leftrightharpoons \frac{6}{11}TiSO_5$	0.181	1.94	0.0874	40.8
94th	$4FeS + \frac{2}{3}FeS_2 + O_2 \leftrightharpoons 2FeO + \frac{8}{3}FeS_2$	0.0279	0.0907	0.0257	39.5

Continued on next page

Place	Transition	Probability of crossing	Price $/kg	Oxygen transfer capacity	Score
95th	$\frac{1}{3}As_2O_3 + \frac{2}{3}As_2S_3 + O_2 \leftrightharpoons \frac{1}{2}As_2S_3 + \frac{1}{2}As_2SO_6$	0.195	0.920	0.0372	39.5
96th	$\frac{5}{8}CuO + \frac{1}{8}CuN_6 + O_2 \leftrightharpoons \frac{3}{8}CuO + \frac{3}{8}CuN_2O_6$	0.410	4.34	0.0829	39.2
97th	$As_2O_3 + \frac{2}{17}AsN_9 + O_2 \leftrightharpoons As_2O_5 + \frac{2}{17}AsN_9$	0.437	2.08	0.0373	39.2
98th	$As_2O_3 + \frac{2}{5}AsCl_3 + O_2 \leftrightharpoons As_2O_5 + \frac{2}{5}AsCl_3$	0.441	1.66	0.0294	39.1
99th	$\frac{14}{9}As_2O_3 + \frac{14}{9}Fe_2O_3 + O_2 \leftrightharpoons \frac{2}{9}As_2O_3 + \frac{4}{9}Fe_7As_6O_{24}$	0.565	0.910	0.0124	38.6
100th	$4Fe_2O_3 + 4FeSiO_3 + O_2 \leftrightharpoons 6Fe_2O_3 + 4SiO_2$	0.531	0.538	0.007 62	37.6

DEPARTMENT OF PHYSICS
CHALMERS UNIVERSITY OF TECHNOLOGY
Gothenburg, Sweden
www.chalmers.se

CHALMERS
UNIVERSITY OF TECHNOLOGY